

Even Order Explicit Symplectic Geometric Algorithms for Solving Quaternions in Guidance Navigation and Control via Diagonal Padé Approximation and Cayley Transform*

Hong-Yan Zhang[†], Fei Liu, Yu Zhou and Man Liang

School of Information Science and Technology, Hainan Normal University, Haikou 571158, China

Aug. 7, 2024

arXiv:2212.06414v3 [eess.SY] 7 Aug 2024

Abstract

Quaternion kinematical differential equation (QKDE) plays a key role in navigation, control and guidance systems. Although explicit symplectic geometric algorithms (ESGA) for this problem are available, there is a lack of a unified way for constructing high order symplectic difference schemes with configurable order parameter and the fractional interval sampling problem should be treated carefully. We present even order explicit symplectic geometric algorithms to solve the QKDE with diagonal Padé approximation via a four-step strategy. Firstly, the Padé-Cayley lemma is proved and used to simplify the symplectic Padé approximation for the linear Hamiltonian system with infinitesimal symplectic structure. Secondly, both parallel and alternative iterative methods are proposed to construct the symplectic difference schemes with even order accuracy. Thirdly, the symplecticity, orthogonality and invertibility of the single-step transition matrices are proved rigorously. Finally, the explicit symplectic geometric algorithms are designed for both the linear time-invariant and linear time-varying QKDE. The maximum absolute error for solving the QKDE is $\mathcal{O}((t_f - t_0)\tau^{2\ell})$ where τ is the time step, ℓ is the order parameter and $[t_0, t_f]$ is the time span. The linear time complexity and constant space complexity of computation as well as the simple algorithmic structure show that our algorithms are appropriate for real-time applications in aeronautics, astronautics, robotics and so on. The performance of the proposed algorithms are verified and validated by mathematical analysis and numerical simulation.

Keywords: Inertia measurement unit (IMU); Guidance navigation and control; Quaternion kinematical differential equation (QKDE); Symplectic geometric algorithm (SGA); Symplectic difference scheme (SDS); Diagonal Padé approximation; Mirrored Cayley transform

*This work was supported in part by the Hainan Provincial Natural Science Foundation of China under Grant 2019RC199, in part by the specific research fund of The Innovation Platform for Academicians of Hainan Province, and in part by the National Natural Science Foundation of China under Grant 62167003.

[†]Corresponding author, e-mail: hongyan@hainnu.edu.cn

Contents

1	Introduction	2
2	Preliminaries	4
2.1	Symplectic Transition Matrix	4
2.2	Padé Approximation and Symplectic Difference Scheme	4
2.3	Cayley Transform and Euler's Formula	5
3	Symplectic Difference Schemes for QKDE	5
3.1	Relation of Padé Approximation and Cayley Transform	5
3.2	Procedure for Computing $\beta(\ell, c)$	6
3.3	Impacts of parameters ℓ and c on $\beta(\ell, c)$	7
3.4	2ℓ -th order SDS for LTI-QKDE	7
3.5	2ℓ -th order SDS for LTV-QKDE	8
4	Symplectic Geometric Algorithms for QKDE	9
4.1	Algorithms for Computing $\beta(\ell, c)$	9
4.2	Algorithm for Computing Symplectic Transition Matrix	10
4.3	Algorithm for Solving LTI-QKDE	10
4.4	Algorithm for Solving LTV-QKDE	10
4.5	Analysis of Computational Complexity	11
5	Performance Evaluation	12
5.1	Measure of NS and AS	12
5.2	Analysis of Accuracy of EOESGAQKDELTI for LTI-QKDE	13
5.3	Simulation of EOESGAQKDELTV for LTV-QKDE	14
5.3.1	Initial Value $q[0]$ for the QKDE	14
5.3.2	A special LTV-QKDE with AS	15
5.3.3	Simulation of LTV-QKDE with MATLAB Simulink	15
5.4	Discussion	15
6	Conclusions	16
A	Hamiltonian System	17

B Cayley Transform and Its Mirror	17
C Horner's Rule for Computing Polynomials	17

1 Introduction

Quaternions have been widely utilized in aerospace [1–5], aeronautics [6–13], robotics [14–20], computer vision [21] and computer graphics [22]. The comprehensive review of fundamental results about linear quaternion differential equations are presented by Kou & Xia [23] and Kartiwa [24]. The key advantages for quaternions stimulating many researches and applications lie in two facts:

- Geometrical singularity can be avoided when the rotation matrices are parameterized with quaternions instead of Euler angles.
- Multiplications and additions are enough for computing quaternions, which implies that quaternions are appropriate for real-time applications because of low computational complexity.

For the navigation, control and guidance problems, the key issue is to find stable and precise numeric solution to the Robinson's *quaternion kinematical differential equation* (QKDE) [25]

$$\begin{cases} \frac{d\mathbf{q}}{dt} = \frac{1}{2}\mathbf{\Omega}(\boldsymbol{\omega}(t))\mathbf{q}, & t \in [t_0, t_f] \\ \mathbf{q}(t_0) = \mathbf{q}_0 \end{cases} \quad (1)$$

where $\mathbf{q} = [e_0, e_1, e_2, e_3]^T$ is the vector representation of the quaternion \mathbf{q} , $[t_0, t_f]$ is the time span, \mathbf{q}_0 is the initial state, $\boldsymbol{\omega} = [\omega_1(t), \omega_2(t), \omega_3(t)]^T \in \mathbb{R}^{3 \times 1}$ is the angular velocity¹ measured by the *inertial measure unit* (IMU), and $\mathbf{\Omega} = \mathbf{\Omega}(\boldsymbol{\omega}(t))$ is specified by the $\boldsymbol{\omega}$ such that

$$\mathbf{\Omega} = -\mathbf{\Omega}^T = \begin{bmatrix} 0 & -\omega_1 & -\omega_2 & -\omega_3 \\ \omega_1 & 0 & \omega_3 & -\omega_2 \\ \omega_2 & -\omega_3 & 0 & \omega_1 \\ \omega_3 & \omega_2 & -\omega_1 & 0 \end{bmatrix}. \quad (2)$$

If the $\boldsymbol{\omega}(t)$ is time independent, then the equation (1) can be called *autonomous* QKDE (A-QKDE) or *linear time-invariant* QKDE (LTI-QKDE) since it is an autonomous system in the sense of classic mechanics and control theory and also it is a linear time-invariant (LTI) system in the sense of signals analysis. On the contrary, if $\boldsymbol{\omega}(t)$ is time dependent, the equation (1) can be named with the *non-autonomous* QKDE (NA-QKDE) or *linear time-varying* QKDE (LTV-QKDE) in general. Although the QKDE (1) is a linear ordinary differential equation (ODE), it is challenging to find its solution for two reasons:

¹In references of aerospace and aeronautics, the notation $\boldsymbol{\omega} = [p, q, r]^T$ is used. In this paper, we use p_i and q_i to denote the i -th generalized momentum and displacement.

- The time-varying vector $\boldsymbol{\omega}(t)$ leads to a time-dependent matrix $\mathbf{\Omega}(\boldsymbol{\omega}(t))$. However, there is no general method for finding the *analytical solution* (AS) to a LTV system.
- The QKDE is critically (neutrally) stable and the numerical solution is sensitive to the computational errors [1] because the eigenvalues of $\mathbf{\Omega}$ specified by (2) contain two pure imaginary numbers $\pm j\|\boldsymbol{\omega}\| = \pm j\sqrt{\omega_1^2 + \omega_2^2 + \omega_3^2}$ where $j = \sqrt{-1}$.

Therefore, it is necessary to find a stable and precise integration method in the sense of long term time for solving (1).

In the past decades, although there are various different engineering-oriented *single step* numeric approaches to solve the QKDE, the existing methods are inadequate in three perspectives:

- Serious accumulative computational errors are involved in the traditional non-symplectic methods. The *traditional finite difference scheme* (TFDS) is sensitive to the accumulative computational errors in the sense of long term time. The typical methods include the Taylor series method [1, 26, 27], classic Runge-Kutta method [28–30] and the periodic normalization strategy [15].
- Earlier symplectic method with high computational complexity is not applicable in a real-time way. Compared with the TFDS, the *symplectic difference scheme* (SDS) can avoid accumulative computational errors automatically. Wang [31] compared the Runge-Kutta scheme with SDS. The Gauss-Legendre difference scheme [32, 33], an accurate and implicit Runge-Kutta method, is an *implicit* SDS. However, its computational complexity is $\mathcal{O}(n^2)$ [34] which means that it is not appropriate for real-time applications.
- Low order non-configurable *Explicit symplectic geometric algorithms* (ESGA) with fractional interval sampling is not perfect for controlling moving object high speed and has extra difficulty in hardware implementation. In 2018, Zhang et al [35] proposed two algorithms — the ESGA-I and ESGA-II — for the LTI-QKDE (A-QKDE) and LTV-QKDE (NA-QKDE) respectively, which are not only precise in the sense of long term time, but also with linear time computational complexity and constant space computational complexity. However, there are some disadvantages for these two algorithms:

- they are not constructed with a unified way and can not be generalized for higher order cases for solving the QKDE with single step approach;
- the discrete time sequence corresponding to the interval $[t_0, t_f]$ is $\left\{t_0, t_0 + \frac{\tau}{2}, \dots, t_0 + \frac{(2k+1)\tau}{2}, \dots\right\}$

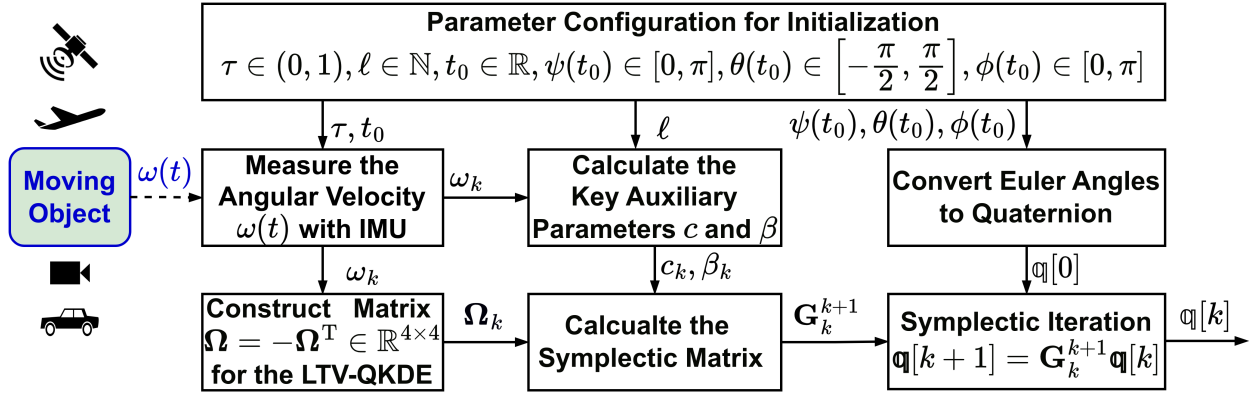


Figure 1: Flow chart of the EoESGA for solving the LTV-QKDE with accuracy parameter ℓ .

instead of $\{t_0, t_0 + \tau, \dots, t_0 + k\tau, \dots\}$ which implies that we have to treat the time intervals carefully;

- iii) the order of the SDS's accuracy is not configurable and high order SDS is missing for moving objects with high speed such as missiles and fourth-generation or fifth-generation fighters.

In consequence, it is necessary for us to explore reconfigurable high order ESGA which could avoid the dark sides i), ii) and iii) mentioned above.

It should be remarked that the accuracy of the measurement of angular velocity $\omega(t)$ is of significant for the algorithms proposed for solving the LTI-QKDE and LTV-QKDE. In other words, the sensors for inertial measurement unit (IMU) is essential for practical applications. Recently, the quantum sensors have been invented for the IMU [36–38]. It could be believed that the accuracy of measuring angular velocity will be wonderful in the near future.

We remark that the theoretic exploring for solving the QKDE is still active in recent years. For example, Cai & Kou proposed the two-sided coefficients method [39], Donachali & Jafari [40] proposed the Adomian decomposition method, Liu et al. [41] discussed QKDE in the perspective of solvability and Green's function. These discussions are not our emphasis since they are not engineering-oriented.

The main purpose of this paper is to propose *even order explicit symplectic geometric algorithms* (EoESGA) for solving the QKDE with Padé approximation and Cayley transform based on the theorems proved for the purpose of engineering applications instead of pure theoretic exploration. The flow chart of solving the LTV-QKDE with the EoESGA via Padé approximation and mirrored Cayley transform is given in **Figure 1**. There are six key steps for solving the LTV-QKDE with the EoESGA parameterized by the integer ℓ , which will be discussed in the following sections.

The contents of this paper are organized as follows: The preliminaries are given in Section 2. Section 3 deals with the SDS for the QKDE. In Section 4 we design the SGA and analyze the computational complexity. Section 5 deals

with performance evaluations. Finally, Section 6 presents the conclusions.

In order to help the reader to recognize the abbreviations, the nomenclatures are summarized in **Table 1**.

Table 1: Nomenclatures

Abbreviation	Interpretation
QKDE	quaternion kinematical differential equation
IMU	inertial measure unit
A-QKDE	autonomous QKDE, or LTI-QKDE
NA-QKD	non-autonomous QKDE, or LTV-QKDE
LTI-QKDE	linear time-invariant QKDE
LTV-QKDE	linear time-varying QKDE
TFDS	traditional finite difference scheme
SDS	symplectic difference scheme
AS	analytical solution
NS	numerical solution
SGA	symplectic geometric algorithm
ESGA	explicit symplectic geometric algorithm
EoESGA	even order ESGA
DPA	diagonal Padé approximation
TCVC	time complexity vector of computation

2 Preliminaries

2.1 Symplectic Transition Matrix

Let τ be the time step and $\mathbf{z}[k] = \mathbf{z}(t_0 + k\tau)$ be the sample value at the discrete time $t_k = t_0 + k\tau$. The SDS for the Hamiltonian canonical equation, see Appendix A and (82), is given by

$$\begin{cases} \mathbf{z}[k+1] = \mathcal{G}_\tau(\mathbf{z}[k]), & k = 0, 1, 2, \dots \\ \mathbf{z}[0] = [p_1(t_0), \dots, p_N(t_0), q_1(t_0), \dots, q_N(t_0)]^\top \end{cases} \quad (3)$$

where $\mathbf{z}[0]$ is the initial condition, $\mathcal{G}_\tau : \mathbb{R}^{2N \times 1} \rightarrow \mathbb{R}^{2N \times 1}$ is the *transition operator*, also named as the *transition mapping*, and

$$\mathbf{G}_k^{k+1}(\tau) = \frac{\partial \mathbf{z}[k+1]}{\partial \mathbf{z}[k]} = \frac{\partial(\mathcal{G}_\tau \mathbf{z}[k])}{\partial \mathbf{z}[k]} \in \mathbb{R}^{2N \times 2N}, \quad (4)$$

is the *transition matrix* (Jacobi matrix) of \mathcal{G}_τ at $\mathbf{z}[k]$ such that $\mathbf{G}_k^{k+1}(\tau)$ is symplectic, viz.,

$$\mathbf{G}_k^{k+1}(\tau)^\top \cdot \mathbf{J}_{2N} \cdot \mathbf{G}_k^{k+1}(\tau) = \mathbf{J}_{2N}. \quad (5)$$

The key problem of designing SGA is to determine the \mathcal{G}_τ or the corresponding Jacobi matrix $\mathbf{G}_k^{k+1}(\tau)$ defined by (4). In this paper, we have $\mathcal{G}_\tau = \mathbf{G}_k^{k+1}(\tau)$ since (1) is a linear ODE. For the SDS of LTI-QKDE, the notation $\mathbf{G}_k^{k+1}(\tau)$ will be replaced by $\mathbf{G}(\tau)$ since it does not depend on the time index k . In this paper, we will also take the notations $\mathbf{G}_k^{k+1}(\ell, \tau)$ and $\mathbf{G}(\ell, \tau)$ where ℓ is the order parameter for accuracy.

2.2 Padé Approximation and Symplectic Difference Scheme

For non-negative integers ℓ and m , the $(\ell + m)$ -th order Padé approximation to $\exp(x)$ is defined by [42–44]

$$\exp(x) = \frac{N_{\ell m}(x)}{D_{\ell m}(x)} + \mathcal{O}(|x|^{\ell+m+1}) \quad (6)$$

where

$$\begin{cases} N_{\ell m}(x) = \sum_{k=0}^m \frac{(\ell+m-k)!m!}{(\ell+m)!k!(m-k)!} x^k, \\ D_{\ell m}(x) = \sum_{k=0}^m \frac{(\ell+m-k)! \ell!}{(\ell+m)!k!(\ell-k)!} (-x)^k. \end{cases} \quad (7)$$

The *diagonal Padé approximation* (DPA) is specified by the condition $\ell = m$, namely

$$\exp(x) = \frac{N_{\ell \ell}(x)}{D_{\ell \ell}(x)} + \mathcal{O}(|x|^{2\ell+1}) \quad (8)$$

where

$$\begin{cases} N_{\ell \ell}(x) = \sum_{k=0}^{\ell} \frac{(2\ell-k)! \ell!}{(2\ell)!k!(\ell-k)!} x^k \\ D_{\ell \ell}(x) = \sum_{k=0}^{\ell} \frac{(2\ell-k)! \ell!}{(2\ell)!k!(\ell-k)!} (-x)^k. \end{cases} \quad (9)$$

Let

$$P_\ell(x) = \sum_{k=0}^{\ell} \frac{(2\ell-k)!}{(2\ell)!} \cdot \frac{\ell!}{(\ell-k)!} \cdot \frac{x^k}{k!}, \quad (10)$$

then both the nominator $N_{\ell \ell}(x)$ and denominator $D_{\ell \ell}(x)$ can be expressed by the $P_\ell(x)$, namely,

$$N_{\ell \ell}(x) = P_\ell(x), D_{\ell \ell}(x) = P_\ell(-x). \quad (11)$$

Simple algebraic operations on factorials show that

$$\begin{aligned} P_\ell(x) &= 1 + \sum_{k=1}^{\ell} \frac{(2\ell-k)!}{(2\ell)!} \cdot \frac{\ell!}{(\ell-k)!} \cdot \frac{x^k}{k!} \\ &= 1 + \sum_{k=0}^{\ell-1} x^{k+1} \prod_{r=0}^k \frac{\ell-r}{(2\ell-r)(r+1)} \end{aligned} \quad (12)$$

It should be pointed out that the factorials in (10) for $k=0$ has been removed in (12) in order to avoid the overflow problem in numerical computations when $2\ell > 10$. Put

$$\eta_r^\ell = \frac{\ell-r}{(2\ell-r)(r+1)}, \quad r \in \{0, 1, \dots, \ell-1\}, \quad (13)$$

then we can obtain

$$P_\ell(x) = 1 + \sum_{k=0}^{\ell-1} x^{k+1} \prod_{r=0}^k \eta_r^\ell \quad (14)$$

Given the parameter ℓ , (14) can be used to generate the expression of $P_\ell(x)$. For illustration, we have

$$\begin{cases} P_1(x) = 1 + \frac{x}{2} \\ P_2(x) = 1 + \frac{x}{2} + \frac{x^2}{12} \\ P_3(x) = 1 + \frac{x}{2} + \frac{x^2}{10} + \frac{x^3}{120} \\ P_4(x) = 1 + \frac{x}{2} + \frac{3x^2}{28} + \frac{x^3}{84} + \frac{x^4}{1680} \\ P_5(x) = 1 + \frac{x}{2} + \frac{x^2}{9} + \frac{x^3}{72} + \frac{1008}{30240} + \frac{x^5}{30240} \\ P_6(x) = 1 + \frac{x}{2} + \frac{5x^2}{44} + \frac{x^3}{66} + \frac{x^4}{792} + \frac{x^5}{15840} + \frac{x^6}{665280} \end{cases} \quad (15)$$

with the help of (13) and (14).

Let

$$g_{\text{DPA}}^\ell(x) = \frac{N_{\ell \ell}(x)}{D_{\ell \ell}(x)} = \frac{P_\ell(x)}{P_\ell(-x)} \quad (16)$$

then the DPA can be written by

$$\exp(x) \sim g_{\text{DPA}}^\ell(x) + \mathcal{O}(|x|^{2\ell+1}) \quad (17)$$

according to (8) and (9). The function $g_{\text{DPA}}^\ell(x)$ for approximating the $\exp(x)$ can be used to construct the SDS of interest. Actually, we have the following theorem [44].

Theorem 1. For the linear Hamiltonian system

$$\frac{dz}{dt} = \mathbf{F}z, \quad \mathbf{F} = \mathbf{J}^{-1}\mathbf{C}, \quad \mathbf{C}^T = \mathbf{C}, \quad (18)$$

where $\mathbf{F} = \mathbf{J}^{-1}\mathbf{C}$ is infinitesimal symplectic, i.e.,

$$\mathbf{J}\mathbf{F} + \mathbf{F}^T\mathbf{J} = \mathbf{O}. \quad (19)$$

Let

$$g_{\text{DPA}}^\ell(\tau\mathbf{F}) = P_\ell(\tau\mathbf{F})[P_\ell(-\tau\mathbf{F})]^{-1} \quad (20)$$

by replacing the symbol x in (17) with the matrix $\tau\mathbf{F}$, then the difference schemes

$$z[k+1] = g_{\text{DPA}}^\ell(\tau\mathbf{F})z[k], \quad \ell = 1, 2, \dots \quad (21)$$

are symplectic of 2ℓ -th order accuracy for step size τ .

2.3 Cayley Transform and Euler's Formula

We now cite two lemmas about mirrored Cayley transform and Euler's formula proved in [35].

Lemma 2 (Generalized Euler's formula). Suppose matrix $\mathbf{M} \in \mathbb{R}^{n \times n}$ is skew-symmetric, i.e., $\mathbf{M}^T = -\mathbf{M}$, and there exists a positive constant γ such that $\mathbf{M}^2 = -\gamma^2\mathbf{I}$. Let $\hat{\mathbf{M}} = \gamma^{-1}\mathbf{M}$, then $\hat{\mathbf{M}}^2 = -\mathbf{I}$. For any $y \in \mathbb{R}$, we have

$$e^{y\mathbf{M}} = \cos(y\gamma)\mathbf{I} + \sin(y\gamma)\hat{\mathbf{M}}. \quad (22)$$

Lemma 3 (Cayley-Euler formula). Suppose matrix $\mathbf{M} \in \mathbb{R}^{n \times n}$ is skew-symmetric, i.e., $\mathbf{M}^T = -\mathbf{M}$, and there exists a positive constant γ such that $\mathbf{M}^2 = -\gamma^2\mathbf{I}$. Let $\hat{\mathbf{M}} = \gamma^{-1}\mathbf{M}$, then $\hat{\mathbf{M}}^2 = -\mathbf{I}$. Let

$$\varphi_{\text{mct}}(\lambda) = \frac{1+\lambda}{1-\lambda} = (1+\lambda)(1-\lambda)^{-1} \quad (23)$$

be the mirrored Cayley transform, then for any $y \in \mathbb{R}$ the Cayley-Euler formula

$$\begin{aligned} \varphi_{\text{mct}}(y\mathbf{M}) &= \frac{\mathbf{I} + y\mathbf{M}}{\mathbf{I} - y\mathbf{M}} = \frac{1}{1+\alpha}[(1-\alpha)\mathbf{I} + 2y\mathbf{M}] \\ &= \cos \delta(y, \gamma)\mathbf{I} + \sin \delta(y, \gamma)\hat{\mathbf{M}} \\ &= e^{\delta(y, \gamma)\mathbf{M}} \end{aligned} \quad (24)$$

holds, in which

$$\begin{cases} \delta = \delta(y, \gamma) = 2 \cdot \arctan(y\gamma) \\ \alpha = \alpha(y, \gamma) = y^2\gamma^2 \end{cases} \quad (25)$$

Furthermore, $\varphi_{\text{mct}}(y\mathbf{M})$ is an orthogonal matrix.

For more information about the mirrored Cayley transform and its properties, please see the Appendix B.

3 Symplectic Difference Schemes for QKDE

3.1 Relation of Padé Approximation and Cayley Transform

Generally, the Padé approximation involves the ratio of polynomials with the same order. It is interesting that the expression of Padé approximation can be simplified into the mirrored Cayley transform for solving the QKDE. We now prove some interesting lemmas and theorems for constructing the SDS for LTI-QKDE.

Lemma 4 (Padé-Cayley). If there exists some positive constant c such that $x^2 = -c$, then each diagonal Padé approximation $g_{\text{DPA}}^\ell(x)$ can be represented by the mirrored Cayley transform

$$g_{\text{DPA}}^\ell(x) = \frac{1 + \beta(\ell, c)x}{1 - \beta(\ell, c)x} = \varphi_{\text{mct}}(\beta(\ell, c)x), \quad (26)$$

where $\beta(\ell, c)$ is a constant determined by ℓ and c .

PROOF: Let $[x] = m$ in which $\exists m \in \mathbb{Z}$ such that $m \leq x < m+1$, and

$$s_1 = \lfloor (\ell-1)/2 \rfloor, \quad s_2 = \lfloor \ell/2 \rfloor, \quad (27)$$

be two integer parameters, we immediately have

$$s_2 = s_1 + 1 - \text{mod}(\ell, 2) = \begin{cases} s_1, & 2 \nmid \ell; \\ s_1 + 1, & 2 \mid \ell. \end{cases} \quad (28)$$

When $x^2 = -c$, equation (12) shows that

$$\begin{aligned} P_\ell(x) &= 1 + \sum_{k=0}^{\ell-1} x^{k+1} \prod_{r=0}^k \eta_r^\ell \\ &= 1 + \sum_{j=0}^{s_1} x^{2j+1} \prod_{r=0}^{2j} \eta_r^\ell + \sum_{j=1}^{s_2} x^{2j} \prod_{r=0}^{2j-1} \eta_r^\ell \\ &= 1 + \sum_{j=1}^{s_2} (-c)^j \prod_{r=0}^{2j-1} \eta_r^\ell + x \sum_{j=0}^{s_1} (-c)^j \prod_{r=0}^{2j} \eta_r^\ell. \end{aligned} \quad (29)$$

Let

$$\begin{cases} a_j^\ell = \prod_{r=0}^{2j} \eta_r^\ell, & 0 \leq j \leq s_1 \\ b_j^\ell = \prod_{r=0}^{2j-1} \eta_r^\ell, & 1 \leq j \leq s_2, \\ b_0^\ell = 1, \end{cases} \quad (30)$$

and

$$\begin{cases} n(s_1, x) = \sum_{j=0}^{s_1} a_j^\ell x^j \\ d(s_2, x) = \sum_{j=0}^{s_2} b_j^\ell x^j \end{cases} \quad (31)$$

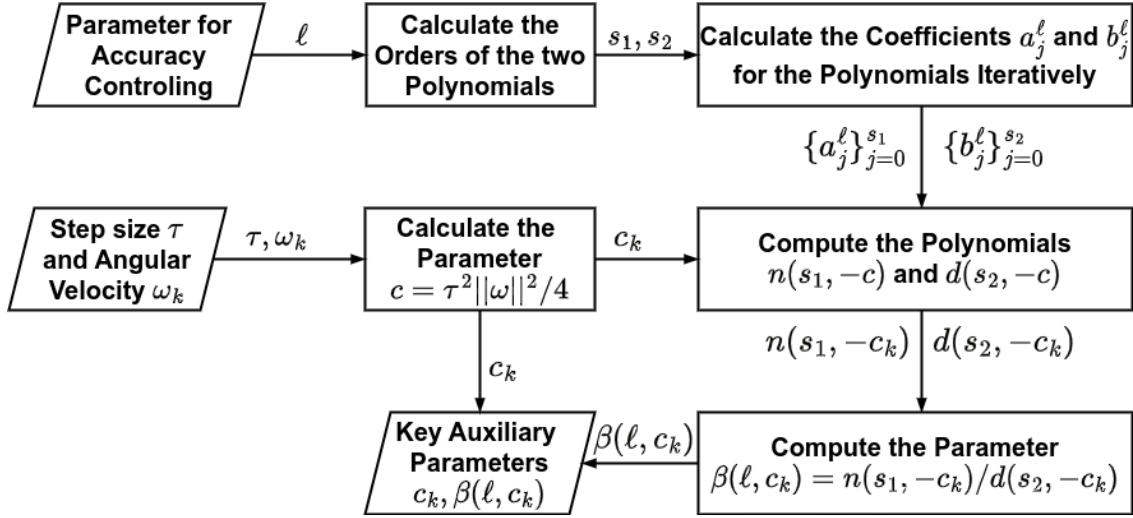


Figure 2: Flow chart of computing the key auxiliary parameters c and β .

By substituting (30) and (31) into (29), we have

$$\begin{aligned}
 P_\ell(x) &= \sum_{j=0}^{s_2} b_j^\ell \cdot (-c)^j + x \sum_{j=1}^{s_1} a_j^\ell \cdot (-c)^j \\
 &= d(s_2, -c) + x \cdot n(s_1, -c).
 \end{aligned} \tag{32}$$

Obviously, (32) is the simplified version of (12) under the condition $x^2 = -c$. Let

$$\beta(\ell, c) = \frac{n(s_1, -c)}{d(s_2, -c)} = \frac{\sum_{j=0}^{s_1} a_j^\ell (-c)^j}{\sum_{j=0}^{s_2} b_j^\ell (-c)^j}, \tag{33}$$

by substituting (32) and (33) into (16), we have

$$\begin{aligned}
 g_{\text{DPA}}^\ell(x) &= \frac{P_\ell(x)}{P_\ell(-x)} = \frac{d(s_2, -c) + x \cdot n(s_1, -c)}{d(s_2, -c) - x \cdot n(s_1, -c)} \\
 &= \frac{1 + \beta(\ell, c)x}{1 - \beta(\ell, c)x} = \varphi_{\text{mct}}(\beta(\ell, c)x).
 \end{aligned} \tag{34}$$

according to (23). Therefore, we can deduce that (26) holds by (17) and (34). Q.E.D.

3.2 Procedure for Computing $\beta(\ell, c)$

The flow chart calculating the auxiliary parameters c and β is illustrated in **Figure 2**. There are two key tasks for computing $\beta(\ell, c)$:

- determine the coefficients a_j^ℓ and b_j^ℓ ;
- calculate the values of polynomials $n(s_1, -c)$ and $d(s_2, -c)$ when c is determined.

For the coefficients of interest, we can use iterative algorithms to generate them. For the computations of polynomials, we can use the famous rule invented by Jiushao Qin

and Horne independently [45–47], see **Algorithm 7** in Appendix C.

There are two typical ways to compute the coefficients a_j^ℓ and b_j^ℓ for the polynomials $n(s_1, -c)$ and $d(s_2, -c)$.

- 1) **Parallel Iterative method:** According to the definition of a_j^ℓ , we can find the following iterative formulas for the coefficients a_j^ℓ :

$$\begin{cases} a_{j+1}^\ell = a_j^\ell \cdot \eta_{2j+1}^\ell \cdot \eta_{2j+2}^\ell, & 0 \leq j \leq s_1 - 1; \\ a_0^\ell = \frac{1}{2}. \end{cases} \tag{35}$$

Similarly, we can obtain

$$\begin{cases} b_{j+1}^\ell = b_j^\ell \cdot \eta_{2j}^\ell \cdot \eta_{2j+1}^\ell, & 0 \leq j \leq s_2 - 1 \\ b_0^\ell = 1. \end{cases} \tag{36}$$

- 2) **Alternative Iterative Method:** We can also obtain the following alternative iterative formula for the coefficients a_j^ℓ and b_j^ℓ

$$\begin{cases} b_0^\ell = 1, \\ a_0^\ell = \frac{1}{2}, \\ b_{j+1}^\ell = a_j^\ell \cdot \eta_{2j+1}^\ell, & 0 \leq j \leq s_1 - 1 \\ a_{j+1}^\ell = b_{j+1}^\ell \cdot \eta_{2j+2}^\ell, & 0 \leq j \leq s_1 - 1 \\ b_{s_2}^\ell = a_{s_1}^\ell \cdot \eta_{2s_1+1}^\ell, & \text{for even } \ell. \end{cases} \tag{37}$$

It is easy to find that the computations in alternative iterative formula (37) are more efficient than those in (35) and (36) since only η_{2j+1}^ℓ and η_{2j+2}^ℓ will be computed.

The iterative algorithms for generating a_j^ℓ and b_j^ℓ are shown in Figure 3. We can find some interesting facts from this figure:

- The structures of the graph for odd ℓ and even ℓ are different. If ℓ is even, then $s_2 = s_1 + 1 = \ell/2$ by (28) and we need an extra iterative step from $a_{s_1}^\ell$ to $b_{s_2}^\ell$ when compared with the case of odd ℓ .

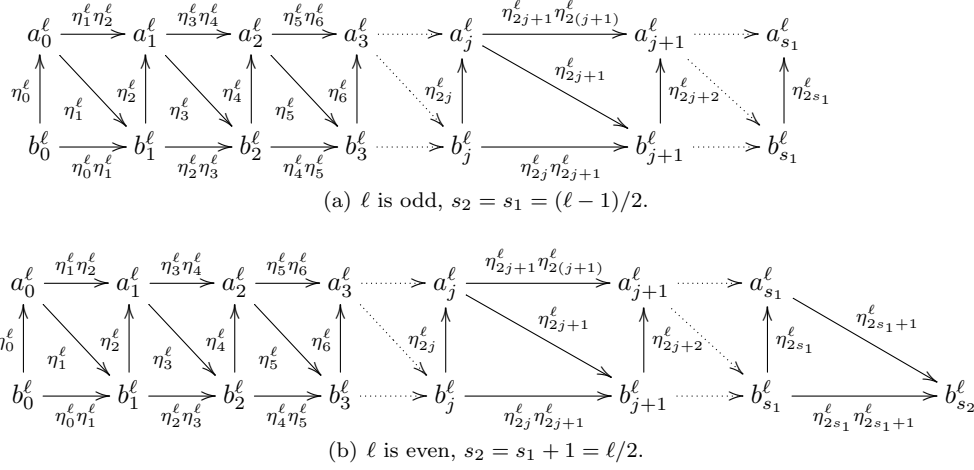


Figure 3: Iterative processes for calculating the coefficients a_j^ℓ and b_j^ℓ correspond to paths on graph.

- For the parallel iterative method, the paths for computing $\{a_j^\ell\}_{j=0}^{s_1}$ and $\{b_j^\ell\}_{j=0}^{s_2}$ are $a_0^\ell \rightarrow a_1^\ell \rightarrow \dots \rightarrow a_j^\ell \rightarrow \dots \rightarrow a_{s_1}^\ell$ and $b_0^\ell \rightarrow b_1^\ell \rightarrow \dots \rightarrow b_j^\ell \rightarrow \dots \rightarrow b_{s_2}^\ell$ respectively. It is obvious that these two paths are independent and the computations involves lots of the products $\eta_{2j+1}^\ell \eta_{2j+2}^\ell$ and $\eta_{2j}^\ell \eta_{2j+1}^\ell$.
- For the alternative iterative method, the path for computing the coefficients of interest is $b_0^\ell \rightarrow a_0^\ell \rightarrow b_1^\ell \rightarrow a_1^\ell \rightarrow \dots \rightarrow b_j^\ell \rightarrow a_j^\ell \rightarrow \dots \rightarrow b_{s_1}^\ell \rightarrow a_{s_1}^\ell \rightarrow b_{s_2}^\ell$ when ℓ is even or $b_0^\ell \rightarrow a_0^\ell \rightarrow b_1^\ell \rightarrow a_1^\ell \rightarrow \dots \rightarrow b_j^\ell \rightarrow a_j^\ell \rightarrow \dots \rightarrow b_{s_1}^\ell \rightarrow a_{s_1}^\ell$ when ℓ is odd.

With the help of a_j^ℓ and b_j^ℓ , we can find the expression of $\beta(\ell, c)$ with fixed ℓ . For $1 \leq \ell \leq 6$, the $\beta(\ell, c)$ are illustrated in **Table 2**. Obviously, $\beta(1, c) \equiv 1/2$ does not depend on the constant c . The series expansion of $\beta(\ell, c)$ at $c = 0$ are also demonstrated in **Table 2**.

3.3 Impacts of parameters ℓ and c on $\beta(\ell, c)$

It is obvious that the transition matrix $\mathbf{G}_k^{k+1}(\ell, \tau)$ depends on the order parameter ℓ by the value of $\beta(\ell, c)$ essentially. Some expressions of $\beta(\ell, c)$ for $1 \leq \ell \leq 6$ are demonstrated in **Table 2**. Note that for different ℓ , the function $\beta(\ell, c)$ will have different domain of convergence (DOC) for parameter c .

Figure 4 illustrates the $\beta(\ell, c)$ for different ℓ and c . **Figure 4(a)** shows that for $c \leq 1.0 \times 10^{-2}$ we have $\beta(\ell, c) \approx \beta(1, c) = \frac{1}{2}$. However, for $c \geq 0.1$, $\beta(\ell, c)$ varies with c significantly. Moreover, for $\ell \geq 4$, $\beta(\ell, c)$ has stable values for any c , which implies that $\ell \geq 4$ will be a satisfactory order parameter. Note that ℓ is a discrete variable and we use continuous lines for visualization in **Figure 4(a)**. On the other hand, **Figure 4(b)** shows that for $\beta(\ell, c)$ differs a lot when $c > 2.0$. Moreover, for $\ell \geq 4$, the $\beta(\ell, c)$ coincides well for any c . In general, it is a good choice for us to set $\ell = 4$ if we prefer high order algorithm.

3.4 2ℓ -th order SDS for LTI-QKDE

Lemma 5. *The diagonal Padé approximation of order ℓ for the transition matrix for the LTI-QKDE is*

$$g_{\text{DPA}}^\ell \left(\frac{\tau}{2} \mathbf{\Omega} \right) = \varphi_{\text{mct}} \left(\beta(\ell, c) \frac{\tau}{2} \mathbf{\Omega} \right) = \frac{\mathbf{I} + \beta(\ell, c) \frac{\tau}{2} \mathbf{\Omega}}{\mathbf{I} - \beta(\ell, c) \frac{\tau}{2} \mathbf{\Omega}} \quad (38)$$

where

$$c = \|\boldsymbol{\omega}\|^2 \tau^2 / 4. \quad (39)$$

PROOF: Equation (39) implies that $(\tau \mathbf{\Omega} / 2)^2 = -c \mathbf{I}$. Thus by Lemma 4 we can find that (38) holds.

Theorem 6. *For any time step τ and time-invariant vector $\boldsymbol{\omega}$, the transition matrix for the LTI-QKDE is*

$$\begin{aligned} \mathbf{G}(\ell, \tau) &= g_{\text{DPA}}^\ell \left(\frac{\tau}{2} \mathbf{\Omega} \right) \\ &= \frac{1}{1 + \alpha(\ell, c)} [(1 - \alpha(\ell, c)) \mathbf{I} + \tau \beta(\ell, c) \mathbf{\Omega}] \\ &= \cos \delta(\ell, \boldsymbol{\omega}, \tau) \mathbf{I} + \sin \delta(\ell, \boldsymbol{\omega}, \tau) \hat{\boldsymbol{\Omega}}, \end{aligned} \quad (40)$$

in which

$$\begin{cases} \alpha(\ell, c) = c[\beta(\ell, c)]^2, \\ \delta(\ell, \boldsymbol{\omega}, \tau) = 2 \arctan(\beta(\ell, c) \|\boldsymbol{\omega}\| \tau / 2), \\ \hat{\boldsymbol{\Omega}} = \mathbf{\Omega} / \|\boldsymbol{\omega}\|, \\ \hat{\boldsymbol{\Omega}}^2 = -\mathbf{I}. \end{cases} \quad (41)$$

PROOF: Let

$$y = \tau \beta(\ell, c) / 2, \quad \gamma = \|\boldsymbol{\omega}\|, \quad \delta = 2 \arctan(y \gamma),$$

then $\mathbf{\Omega}^2 = -\gamma^2 \mathbf{I}$ and

$$\alpha(\ell, c) = y^2 \gamma^2 = c[\beta(\ell, c)]^2.$$

Let $\mathbf{M} = \mathbf{\Omega}$, then this theorem follows from the Lemma 3 directly. Q.E.D.

Table 2: Expressions of $\beta(\ell, c)$ for $1 \leq \ell \leq 6$

ℓ	$\beta(\ell, c) = \frac{n(s_1, -c)}{d(s_2, -c)}$	Taylor series of $\beta(\ell, c)$ at $c = 0$	DOC
1	$\frac{1}{2}$	$\frac{1}{2}$	$[0, +\infty)$
2	$\frac{\frac{1}{2}}{1 - \frac{1}{12}c}$	$\frac{1}{2} + \frac{c}{24} + \frac{c^2}{288} + \frac{c^3}{3456} + \frac{c^4}{41472} + \frac{c^5}{497664} + \frac{c^6}{5971968} + \mathcal{O}(c^7)$	$[0, 12)$
3	$\frac{\frac{1}{2} - \frac{1}{120}c}{1 - \frac{1}{10}c}$	$\frac{1}{2} + \frac{c}{24} + \frac{c^2}{240} + \frac{c^3}{2400} + \frac{c^4}{24000} + \frac{c^5}{240000} + \frac{c^6}{2400000} + \mathcal{O}(c^7)$	$[0, 10)$
4	$\frac{\frac{1}{2} - \frac{1}{84}c}{1 - \frac{3}{28}c + \frac{1}{1680}c^2}$	$\frac{1}{2} + \frac{c}{24} + \frac{c^2}{240} + \frac{17c^3}{40320} + \frac{241c^4}{5644800} + \frac{41c^5}{9483264} + \frac{29063c^6}{6638284800} + \mathcal{O}(c^7)$	$\left[0, \frac{12650}{1281}\right)$
5	$\frac{\frac{1}{2} - \frac{1}{72}c + \frac{1}{30240}c^2}{1 - \frac{1}{9}c + \frac{1}{1008}c^2}$	$\frac{1}{2} + \frac{c}{24} + \frac{c^2}{240} + \frac{17c^3}{40320} + \frac{31c^4}{725760} + \frac{1583c^5}{365783040} + \frac{2887c^6}{6584094720} + \mathcal{O}(c^7)$	$\left[0, \frac{2349}{238}\right)$
6	$\frac{\frac{1}{2} - \frac{1}{66}c + \frac{1}{15840}c^2}{1 - \frac{5}{44}c + \frac{1}{792}c^2 - \frac{1}{665280}c^3}$	$\frac{1}{2} + \frac{c}{24} + \frac{c^2}{240} + \frac{17c^3}{40320} + \frac{31c^4}{725760} + \frac{691c^5}{159667200} + \frac{388151c^6}{885194956800} + \mathcal{O}(c^7)$	$\left[0, \frac{10294}{1043}\right)$

Theorem 7. For any $\ell \in \mathbb{N}$, constant $\omega \in \mathbb{R}^{3 \times 1}$ and any $\tau \in \mathbb{R}$, the transition matrix $\mathbf{G}(\ell, \tau)$ is an orthogonal, invertible and symplectic transformation with 2ℓ -th order accuracy, i.e.,

$$\mathbf{G}(\ell, \tau)^{-1} = \mathbf{G}(\ell, -\tau) = \mathbf{G}(\ell, \tau)^T \quad (42)$$

for the LTI-QKDE.

PROOF: For a time-invariant vector ω , the function $\delta(\ell, \omega, \tau)$ is an odd function of τ . With the help of $\hat{\Omega}^2 = -\mathbf{I}$ and $\hat{\Omega}^T = -\hat{\Omega}$, we immediately obtain

$$\begin{aligned} \mathbf{G}(\ell, \tau)^T &= [\cos \delta(\ell, \omega, \tau)\mathbf{I} + \sin \delta(\ell, \omega, \tau)\hat{\Omega}]^T \\ &= \cos(-\delta(\ell, \omega, \tau))\mathbf{I} + \sin(-\delta(\ell, \omega, \tau))\hat{\Omega} \\ &= \mathbf{G}(\ell, -\tau), \end{aligned}$$

which implies that the transition matrix is invertible. Moreover, $\mathbf{G}(\ell, \tau)$ is orthogonal by Lemma 3. In consequence, $\mathbf{G}(\ell, \tau)^T = \mathbf{G}(\ell, -\tau) = \mathbf{G}(\ell, \tau)^{-1}$.

Since the $\mathbf{G}(\ell, \tau)$ is constructed from the Padé approximation $g_{\text{DPA}}^\ell(\cdot)$ directly according to Theorem 1, it must be a SDS with 2ℓ -th order accuracy. Q.E.D.

3.5 2ℓ -th order SDS for LTV-QKDE

For the time-varying vector $\omega(t)$, the LTV-QKDE is a non-autonomous Hamiltonian system essentially and the

corresponding SGA can be obtained via the concept of extended phase space and time-centered difference scheme (See [44], Chapter 5). Let $\bar{t}_k = t[k] + \tau/2$, $\omega_k = \omega(\bar{t}_k)$, $\Omega_k = \Omega(\omega_k)$ with the similar procedure as we do in finding the transition matrix for SDS of the LTI-QKDE. However, we have to treat the discrete time sequence $t_0, t_0 + \frac{\tau}{2}, t_0 + \frac{3\tau}{2}, \dots, t_0 + \frac{(2k+1)\tau}{2}, t_0 + \frac{(2k+3)\tau}{2}, \dots$ and the corresponding symplectic transition matrices $\mathbf{G}_k^{k+1}(\cdot)$ at these discrete time. Thus we have to treat the initial condition $\mathbf{q}(t_0)$ carefully since the length of interval $[t_0, t_0 + \frac{\tau}{2}]$ is not equal to that of $[t_0 + \frac{(2k+1)\tau}{2}, t_0 + \frac{(2k+3)\tau}{2}]$. In order to avoid this phenomena and the fractional sampling problem, we use the following modified version of the discrete vectors ω_k and matrices Ω_k

$$\omega_k = \omega(t[k]), \quad \Omega_k = \Omega(\omega_k), \quad (43)$$

thus we can obtain the k -th transition matrix at time $t[k]$

$$\mathbf{G}_k^{k+1}(\ell, \tau) = g_\ell(\tau\Omega_k/2) = \phi(\beta(\ell, c_k)\tau\Omega_k/2) \quad (44)$$

for the LTV-QKDE. By Lemma 3, it is easy to prove the following theorem.

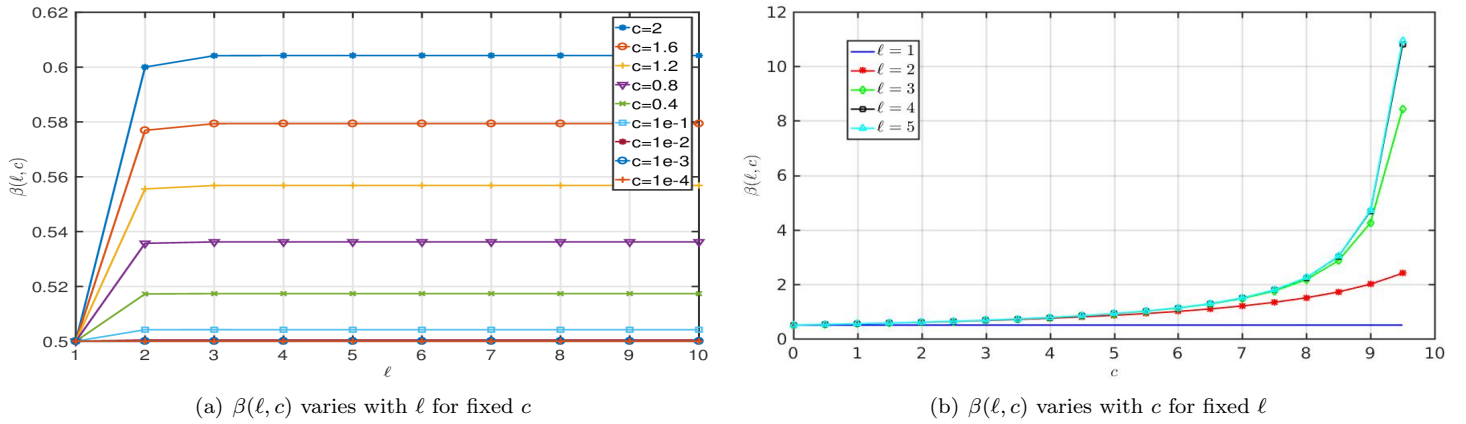


Figure 4: Impact of ℓ and c on $\beta(\ell, c)$

Theorem 8. For the LTV-QKDE $\frac{d\mathbf{q}}{dt} = \frac{1}{2}\mathbf{\Omega}[\boldsymbol{\omega}(t)]\mathbf{q}$, let

$$\begin{cases} c_k = \tau^2 \|\boldsymbol{\omega}_k\|^2 / 4 \\ \beta_k = \beta(\ell, c_k) \\ \alpha_k^\ell = \alpha(\ell, c_k) = c_k \beta_k^2 \end{cases} \quad (45)$$

then the transition matrices $\mathbf{G}_k^{k+1}(\ell, \tau) : \mathbf{q}[k] \mapsto \mathbf{q}[k+1]$ can be expressed by

$$\begin{aligned} \mathbf{G}_k^{k+1}(\ell, \tau) &= \frac{1}{1 + \alpha(\ell, c_k)} [(1 - \alpha(\ell, c_k)\mathbf{I} + \tau\beta(\ell, c_k)\mathbf{\Omega}_k)] \\ &= \cos[\delta(\ell, \boldsymbol{\omega}_k, \tau)]\mathbf{I} + \sin[\delta(\ell, \boldsymbol{\omega}_k, \tau)]\hat{\boldsymbol{\Omega}}(\boldsymbol{\omega}_k), \end{aligned} \quad (46)$$

which generates a SDS with 2ℓ -th order accuracy for $k = 0, 1, 2, \dots$.

Note that $\mathbf{G}_k^{k+1}(\ell, \tau)$ is also symplectic and orthogonal. However, $\mathbf{G}_k^{k+1}(\ell, -\tau) \neq [\mathbf{G}_k^{k+1}(\ell, \tau)]^{-1}$ since $\boldsymbol{\omega}(t)$ is time-dependent and $\boldsymbol{\omega}(t[k] - \tau) \neq \boldsymbol{\omega}(t[k] + \tau)$ in general.

4 Symplectic Geometric Algorithms for QKDE

4.1 Algorithms for Computing $\beta(\ell, c)$

For the practical computation of $\beta(\ell, c)$, it is necessary to find η_k^ℓ frequently. For the purpose of clarity, we design a simple procedure ETA to compute η_k^ℓ according to (13), see **Algorithm 1**.

Algorithm 1 Compute the Parameter η_k^ℓ

Input: Parameter $\ell \in \mathbb{N}$ for order and integer k .

Output: The value of η_k^ℓ .

- 1: **function** ETA(ℓ, k)
- 2: $\eta_k^\ell \leftarrow \frac{\ell - k}{(2\ell - k)(k + 1)}$;

- 3: **return** η_k^ℓ ;
 - 4: **end function**
-

With the help of **Algorithm 7** in Appendix C, we can design two fast and stable iterative algorithms for generating $\beta(\ell, c)$ according to (33), see **Algorithm 2** and **Algorithm 3**.

Algorithm 2 Parallel Fast and Stable Iterative Algorithm for Generating $\beta(\ell, c)$

Input: Positive integer ℓ and auxiliary parameter c .

Output: Key auxiliary parameter β

- 1: **function** PFSIAGENBETA(ℓ, c)
 - 2: $s_1 \leftarrow \lfloor (\ell - 1)/2 \rfloor, s_2 \leftarrow \lfloor \ell/2 \rfloor$;
 - 3: Allocate memory for $s_1 + 1$ coefficients a_j^ℓ .
 - 4: Allocate memory for $s_2 + 1$ coefficients b_j^ℓ .
 - 5: $a_0^\ell \leftarrow \frac{1}{2}$;
 - 6: **for** ($j \leftarrow 0; j \leq s_1 - 1; j \leftarrow j + 1$) **do**
 - 7: $a_{j+1}^\ell \leftarrow a_j^\ell \cdot \text{ETA}(\ell, 2j + 1) \cdot \text{ETA}(\ell, 2j + 2)$;
 - 8: **end for**
 - 9: $b_0^\ell \leftarrow 1$;
 - 10: **for** ($j \leftarrow 0; j \leq s_2 - 1; j \leftarrow j + 1$) **do**
 - 11: $b_{j+1}^\ell \leftarrow b_j^\ell \cdot \text{ETA}(\ell, 2j) \cdot \text{ETA}(\ell, 2j + 1)$;
 - 12: **end for**
 - 13: $n \leftarrow \text{POLYNOMIAL}(a_0^\ell, \dots, a_{s_1}^\ell, -c)$;
 - 14: $d \leftarrow \text{POLYNOMIAL}(b_0^\ell, \dots, b_{s_2}^\ell, -c)$;
 - 15: $\beta \leftarrow n/d$;
 - 16: **return** β ;
 - 17: **end function**
-

Algorithm 3 Alternative Fast and Stable Iterative Algorithm for Generating $\beta(\ell, c)$

Input: Positive integer ℓ and auxiliary parameter c .

Output: Key auxiliary parameter β

```

1: function AFSGENBETA( $\ell, c$ )
2:    $s_1 \leftarrow \lfloor (\ell - 1)/2 \rfloor, s_2 \leftarrow \lfloor \ell/2 \rfloor;$ 
3:   Allocate memory for  $s_1 + 1$  coefficients  $a_j^\ell$ .
4:   Allocate memory for  $s_2 + 1$  coefficients  $b_j^\ell$ .
5:   Set  $b_0^\ell \leftarrow 1, a_0^\ell \leftarrow \frac{1}{2};$ 
6:   for ( $j \leftarrow 0; j \leq s_1 - 1; j \leftarrow j + 1$ ) do
7:      $b_{j+1}^\ell \leftarrow a_j^\ell \cdot \text{ETA}(\ell, 2j + 1);$ 
8:      $a_{j+1}^\ell \leftarrow b_{j+1}^\ell \cdot \text{ETA}(\ell, 2j + 2);$ 
9:   end for
10:  if  $2 \mid \ell$  then  $b_{s_2}^\ell \leftarrow a_{s_1}^\ell \cdot \text{ETA}(\ell, 2s_1 + 1);$ 
11:  end if
12:   $n \leftarrow \text{POLYNOMIAL}(a_0^\ell, \dots, a_{s_1}^\ell, -c);$ 
13:   $d \leftarrow \text{POLYNOMIAL}(b_0^\ell, \dots, b_{s_2}^\ell, -c);$ 
14:   $\beta \leftarrow n/d;$ 
15:  return  $\beta;$ 
16: end function

```

Note that the computation of a_j^ℓ and b_j^ℓ in **Algorithm** (2) is based on (35) and (36). However, (37) is taken for **Algorithm** (3) by comparison.

4.2 Algorithm for Computing Symplectic Transition Matrix

The symplectic transition matrix $\mathbf{G}_k^{k+1}(\ell, \tau)$ at any time t_k can be computed based on (45) and (46) at time t_k .

Algorithm 4 Symplectic Transition Matrix for LTV-QKDE

Input: Angular velocity $\boldsymbol{\omega} \in \mathbb{R}^{3 \times 1}$ at time t_k , order parameter ℓ and time step τ .

Output: Symplectic transition matrix \mathbf{G} for the LTV-QKDE $\frac{d\mathbf{q}}{dt} = \frac{1}{2}\boldsymbol{\Omega}(\boldsymbol{\omega}(t))\mathbf{q}$ at time t with 2ℓ -th order accuracy.

```

1: function SPTRANMATQKDELTV( $\ell, \tau, \boldsymbol{\omega}$ )
2:   Set matrix  $\boldsymbol{\Omega}$  with  $\boldsymbol{\omega} = \boldsymbol{\omega}(t_k)$ :

```

$$\boldsymbol{\Omega} \leftarrow \begin{bmatrix} 0 & -\omega_1 & -\omega_2 & -\omega_3 \\ \omega_1 & 0 & \omega_3 & -\omega_2 \\ \omega_2 & -\omega_3 & 0 & \omega_1 \\ \omega_3 & \omega_2 & -\omega_1 & 0 \end{bmatrix}$$

```

3:    $c \leftarrow \tau^2 \|\boldsymbol{\omega}\|^2 / 4;$  // by (45)
4:    $\beta \leftarrow \text{AFSGENBETA}(\ell, c);$  // by (45)
5:    $\alpha \leftarrow c\beta^2;$  // by (45)
6:    $\mathbf{G}(\ell, \tau) \leftarrow \frac{1}{1+\alpha} [(1-\alpha)\mathbf{I} + \tau\beta\boldsymbol{\Omega}];$  // by (46)
7:   return  $\mathbf{G}(\ell, \tau);$ 
8: end function

```

It is easy to find that in the Step 4 for computing the $\beta(\ell, c)$, the parallel algorithm PFSIAGENBETA described in **Algorithm 2** is also feasible.

4.3 Algorithm for Solving LTI-QKDE

The 2ℓ -th order ESGA for LTI-QKDE based on Padé approximation, EOESGAQKDELTI for brevity², is given in **Algorithm 5** by the explicit expression of $\mathbf{G}(\ell, \tau)$ via (40). Particularly, if $\ell = 1$, then the $\mathbf{G}(1, \tau)$ is the same with its counterpart in the ESGA-I algorithm proposed in [35] since $\beta(1, c) \equiv \frac{1}{2}$ for any positive number c .

Algorithm 5 2ℓ -th Order Explicit Symplectic Geometric Algorithm for LTI-QKDE

Input: The constant angular velocity vector $\boldsymbol{\omega} \in \mathbb{R}^{3 \times 1}$, time step τ , order parameter ℓ , time interval $[t_0, t_f]$ and the initial state quaternion \mathbf{q}_0 at time t_0 .

Output: Numerical solution to the LTI-QKDE $\frac{d\mathbf{q}}{dt} = \frac{1}{2}\boldsymbol{\Omega}(\boldsymbol{\omega})\mathbf{q}$ for $t_0 \leq t \leq t_f$ with 2ℓ -th order SDS.

```

1: function EOESGAQKDELTI( $\ell, \tau, \boldsymbol{\omega}, \mathbf{q}_0, t_0$ )
2:    $t[0] \leftarrow t_0, \mathbf{q}[0] \leftarrow \mathbf{q}_0;$ 
3:    $\mathbf{G}(\ell, \tau) = \text{SPTRANMATQKDELTV}(\ell, \tau, \boldsymbol{\omega})$ 
4:   for ( $k \leftarrow 0; t[k] < t_f; k \leftarrow k + 1$ ) do
5:      $\mathbf{q}[k + 1] \leftarrow \mathbf{G}(\ell, \tau)\mathbf{q}[k];$ 
6:      $t[k + 1] \leftarrow t[k] + \tau;$ 
7:   end for
8:   return The sequence  $\{\mathbf{q}[k]\};$ 
9: end function

```

Note that for computing $\beta(\ell, c)$ in Step 6 of **Algorithm 5**, we can use PFSIAGENBETA(ℓ, c) or AFSGENBETA for FSIAGENBETA according to the practical engineering requirements. Moreover, if a fixed ℓ is preferred, say $\ell = 4$, we can choose a specific polynomial from Table I. This strategy also holds for **Algorithm 6** in the following subsection.

We remark that for real-time applications, it is not necessary to store the sequences $\{t[k]\}$ and $\{\mathbf{q}[k]\}$. It is enough for us to store the current state $\mathbf{q}[k]$ at time $t[k]$, which implies that we just need to store two real numbers. Obviously, this remark holds for the **Algorithm 6** EOESGAQKDELTV in the following subsection.

4.4 Algorithm for Solving LTV-QKDE

The even order ESGA for LTV-QKDE based on Padé approximation, EOESGAQKDELTV for brevity, is presented in **Algorithm 6**. It should be noted that we can

²“Eo” means *even order* since 2ℓ must be an even integer. We use EOESGAQKDELTI instead of EOESGALTIQKDE since the EOESGAQKDELTI and its counterpart EOESGAQKDELTV can be merged into EOESGAQKDE with function overloading in object-oriented programming.

share some memories for the time-dependent parameters $\boldsymbol{\omega}_k, \boldsymbol{\Omega}_k, c_k, \beta_k^\ell, \alpha_k^\ell$ and $\mathbf{G}_k^{k+1}(\ell, \tau)$ since they are local variables for computing the sequence $\{\mathfrak{q}[k]\}$.

By comparison, EOESGAQKDELTV differs the EOESGAQKDELTI from two points: the angular velocity at time $t[k]$ should be computed and the computation of \mathbf{G} is moved into the loop.

Algorithm 6 2ℓ -th Order Explicit Symplectic Geometric Algorithm for LTV-QKDE

Input: The time-varying vector $\boldsymbol{\omega}(t) \in \mathbb{R}^{3 \times 1}$, positive integer ℓ , time interval $[t_0, t_f]$, initial quaternion \mathfrak{q}_0 and time step τ .

Output: Numeric solution $\{\mathfrak{q}[k]\}$ to the LTV-QKDE $\frac{d\mathfrak{q}}{dt} = \frac{1}{2}\boldsymbol{\Omega}(\boldsymbol{\omega}(t))\mathfrak{q}$ for $t_0 \leq t \leq t_f$ with 2ℓ -th order accuracy.

```

1: function EOESGAQKDELTV( $\ell, \tau, \boldsymbol{\omega}(t), \mathfrak{q}_0, t_0, t_f$ )
2:    $t[0] \leftarrow t_0, \mathfrak{q}[0] \leftarrow \mathfrak{q}_0$ ;
3:   for ( $k \leftarrow 0; t[k] < t_f; k \leftarrow k + 1$ ) do
4:      $\boldsymbol{\omega}_k \leftarrow [\omega_1(t[k]), \omega_2(t[k]), \omega_3(t[k])]^\top$ ;
5:      $\mathbf{G}_k^{k+1}(\ell, \tau) \leftarrow \text{SPTRANMATQKDELTV}(\ell, \tau, \boldsymbol{\omega}_k)$ ;
6:      $\mathfrak{q}[k + 1] \leftarrow \mathbf{G}_k^{k+1}(\ell, \tau)\mathfrak{q}[k]$ ;
7:      $t[k + 1] \leftarrow t[k] + \tau$ ;
8:   end for
9:   return The sequence  $\{\mathfrak{q}[k]\}$ ;
10: end function

```

Note that for the steps in the loop, we can use the notations $\boldsymbol{\omega}_k$ and \mathbf{G}_k^{k+1} for understanding (see Theorem 8). For the implementation of algorithm EOESGAQKDELTV, we can use the notations $\boldsymbol{\omega}$ and \mathbf{G} in order to share memories for the temporary (local) variables in the sense of computer programming.

4.5 Analysis of Computational Complexity

Let $\mathcal{T}_*(\mathbf{expr})$ and $\mathcal{T}_+(\mathbf{expr})$ be the times of multiplication and addition in some operation expression \mathbf{expr} . The *time complexity vector of computation* (TCVC) for \mathbf{expr} is defined by

$$\mathcal{T}(\mathbf{expr}) = [\mathcal{T}_*(\mathbf{expr}), \mathcal{T}_+(\mathbf{expr})]. \quad (47)$$

Note that we just list two components of $\mathcal{T}(\mathbf{expr})$ here since for the problems and algorithms which contain massive matrix-vector operations, the multiplication and addition operations for real numbers are fundamental and essential.

Similarly, we use $T(\mathbf{expr})$ to denote the computation time for \mathbf{expr} . We also use $T_*(\mathbf{expr})$ and $T_+(\mathbf{expr})$ to represent the computation time for the multiplications and additions involved in \mathbf{expr} . Suppose that the time units for multiplication and addition are u_1 and u_2 respectively. Let

$$\mathbf{u} = [u_1, u_2] \quad (48)$$

be the vector of time units. Then the time for computing \mathbf{expr} will be

$$\begin{aligned} T(\mathbf{expr}) &= \langle \mathcal{T}(\mathbf{expr}) | \mathbf{u} \rangle \\ &= \mathcal{T}_*(\mathbf{expr})u_1 + \mathcal{T}_+(\mathbf{expr})u_2 \\ &= T_*(\mathbf{expr}) + T_+(\mathbf{expr}) \end{aligned} \quad (49)$$

if only multiplication and addition are essential for the total time consumed.

For an algorithm named with ALG, its TCVC is defined by

$$\begin{aligned} \mathcal{T}(\text{ALG}) &= \sum_{\mathbf{expr} \in \text{ALG}} \mathcal{T}(\mathbf{expr}) \\ &= [\mathcal{T}_*(\text{ALG}), \mathcal{T}_+(\text{ALG})]. \end{aligned} \quad (50)$$

The time needed for algorithm ALG can be measured by

$$T(\text{ALG}) = \langle \mathcal{T}(\text{ALG}) | \mathbf{u} \rangle = \mathcal{T}_*(\text{ALG})u_1 + \mathcal{T}_+(\text{ALG})u_2 \quad (51)$$

theoretically with acceptable accuracy.

It is easy to check that the TCVC for Algorithm 1 for computing $\eta_k^\ell = \text{ETA}(\ell, k)$ is

$$\mathcal{T}(\text{ETA}) = \sum_{\mathbf{expr} \in \text{ETA}} \mathcal{T}(\mathbf{expr}) = [3, 3]. \quad (52)$$

The TCVC for computing the polynomial $p_s(x) = \sum_{i=0}^s c_i x^i$

via Horne's rule is

$$\mathcal{T}(\text{POLYNOMIAL}) = \sum_{\mathbf{expr} \in \text{POLYNOMIAL}} \mathcal{T}(\mathbf{expr}) = [s, s] \quad (53)$$

Simple algebraic operations show that The TCVC for **Algorithm 2** and **Algorithm 3** are

$$\begin{aligned} &\mathcal{T}(\text{PFSIAGENBETA}) \\ &= \sum_{\mathbf{expr} \in \text{PFSIAGENBETA}} \mathcal{T}(\mathbf{expr}) \\ &= s_1[11, 9] + s_2[11, 8] + [5, 3] \\ &= [11(s_1 + s_2) + 5, 9s_1 + 8s_2 + 3] \\ &= \begin{cases} [11\ell - 6, (17\ell - 11)/2], & \text{for } 2 \nmid \ell; \\ [11\ell - 6, (17\ell - 12)/2], & \text{for } 2 \mid \ell; \end{cases} \\ &= [11\ell - 6, (17\ell - 12 + \text{mod}(\ell, 2))/2], \quad \forall \ell \in \mathbb{N} \end{aligned} \quad (54)$$

and

$$\begin{aligned} \mathcal{T}(\text{AFSIAGENBETA}) &= \sum_{\mathbf{expr} \in \text{AFSIAGENBETA}} \mathcal{T}(\mathbf{expr}) \\ &= [6\ell - 1, 5\ell - 3], \quad \forall \ell \in \mathbb{N} \end{aligned} \quad (55)$$

respectively. Obviously, the time complexity of AFSIAGENBETA is lower than that of PFSIAGENBETA since there is only one loop in the former. However, if we

Table 3: Time and Space Consumptions of EoESGAQKDELTV

Step	TCVC	Numbers/matrices to be stored
0	—	$t_0, t_f, \tau \in \mathbb{R}, \mathfrak{q}[0] \in \mathbb{R}^{4 \times 1}, \ell \in \mathbb{N}$
1	—	—
2	—	$k \in \mathbb{Z}, t[k] \in \mathbb{R}$
3	—	$\boldsymbol{\omega} \in \mathbb{R}^{3 \times 1}$
4	$[6\ell + 29, 5\ell + 6]$	$c, \beta, \alpha \in \mathbb{R}, \mathbf{G} \in \mathbb{R}^{4 \times 4}$
5	$[16, 12]$	$\mathfrak{q}[k + 1] \in \mathbb{R}^{4 \times 1}$
6	$[0, 1]$	—
7	—	—
8	—	—

take parallel programming, the two loops in PFSIAGEN-BETA can be executed at the same time. In this way, the difference of the time complexity will be ignorable.

The TCVC for SPTRANMATQKDE can be expressed by

$$\begin{aligned} \mathcal{J}(\text{SPTRANMATQKDE}) &= \sum_{\text{expr} \in \text{SPTRANMATQKDE}} \mathcal{J}(\text{expr}) \\ &= [6\ell + 29, 5\ell + 6], \quad \forall \ell \in \mathbb{N}. \end{aligned} \quad (56)$$

This implies that the computational cost is constant for fixed ℓ and varies with ℓ linearly when ℓ increases.

Let

$$n = \lfloor (t_f - t_0) / \tau \rfloor, \quad (57)$$

then there are n iterations for the loops in **Algorithm 5** and **Algorithm 6**. **Table 3** shows that the TCVC for EoESGAQKDELTV is

$$\begin{aligned} \mathcal{J}(\text{EoESGAQKDELTV}) &= \sum_{\text{expr} \in \text{EoESGAQKDELTV}} \mathcal{J}(\text{expr}) \\ &= [6\ell n + 45n, 5\ell n + 19n] \end{aligned} \quad (58)$$

and the total time consumed (without optimization) can be measured by

$$\begin{aligned} T(\text{EoESGAQKDELTV}) &= \langle \mathcal{J}(\text{EoESGAQKDELTV}) | \mathbf{u} \rangle \\ &= (6\ell n + 45n)u_1 + (5\ell n + 19n)u_2 \\ &= \mathcal{O}(n) \end{aligned} \quad (59)$$

for fixed order parameter ℓ , time units u_1 and u_2 . By comparison, the TCVC for EoESGAQKDELTI is

$$\begin{aligned} \mathcal{J}(\text{EoESGAQKDELTI}) &= \sum_{\text{expr} \in \text{EoESGAQKDELTI}} \mathcal{J}(\text{expr}) \\ &= [16n + 6\ell + 29, 13n + 5\ell + 6] \end{aligned} \quad (60)$$

and the time consumed will be

$$\begin{aligned} T(\text{EoESGAQKDELTI}) &= \langle \mathcal{J}(\text{EoESGAQKDELTI}) | \mathbf{u} \rangle \\ &= (16n + 6\ell + 29)u_1 + (13n + 5\ell + 6)u_2 \\ &= \mathcal{O}(n). \end{aligned} \quad (61)$$

Therefore, the time complexity for both EoESGAQKDELTI and EoESGAQKDELTV are linear. Moreover, it is necessary to store the global variables t_0, t_f, τ and local variables $\omega_1, \omega_2, \omega_3, \boldsymbol{\Omega}, \alpha, \beta, \mathbf{G}, k$ and $\mathfrak{q}[k]$. The storage sharing mechanics implies that only 45 real numbers as well as a pointer to $\boldsymbol{\omega}(t)$ should be stored in this algorithm for real-time applications. Obviously, the space complexity is constant, i.e., $\mathcal{O}(1)$.

We remark that we can set $\beta(\ell, c)$ according to the **Table 2** without invoking the **Algorithm 2** or **Algorithm 3**. By this way, the time complexity of **Algorithm 5** and **Algorithm 6** will still be linear.

5 Performance Evaluation

The fundamental aspects of verification and validation of ESGA for QKDE are discussed in detail in [35]. Our emphasis here lies in the following issues:

- Analysis of accuracy of EoESGAQKDELTI;
- Verification and evaluation of EoESGAQKDELTV;
 - Comparison of the NS and AS for some special time-varying $\boldsymbol{\omega}(t)$ and $\mathfrak{q}[0]$;
 - Verification of EoESGAQKDELTV with MATLAB Simulink for general case.

5.1 Measure of NS and AS

Let $\mathbf{G}_{\text{AS}}(k, \tau)$ and $\mathbf{G}_{\text{NS}}(k, \tau)$ be the AS and NS to the single step transition matrix at time $t[k]$ respectively. Obviously, we have

$$\mathbf{G}_{\text{AS}}(k, \tau) = \mathbf{G}_k^{k+1}(\tau), \quad \mathbf{G}_{\text{NS}}(k, \tau) = \mathbf{G}_k^{k+1}(\ell, \tau). \quad (62)$$

The error operator of step k is defined by

$$\begin{aligned} \mathbf{E}_{\mathcal{G}}[k] &= \mathbf{G}_{\text{AS}}(k, \tau) - \mathbf{G}_{\text{NS}}(k, \tau) \\ &= \mathbf{G}_k^{k+1}(\tau) - \mathbf{G}_k^{k+1}(\ell, \tau). \end{aligned} \quad (63)$$

For the fixed τ and ℓ , the absolute error of the NS for the k -th solution $\mathfrak{q}[k]$ is

$$\begin{aligned} E_k(\ell, \tau) &= \|\mathfrak{q}_1^{\text{NS}}[k] - \mathfrak{q}_1^{\text{AS}}[k]\| \\ &= \sqrt{\sum_{i=0}^3 |e_i^{\text{AS}}[k] - e_i^{\text{NS}}[k]|^2}. \end{aligned} \quad (64)$$

The maximum absolute error for solving $\mathfrak{q}(t)$ on interval $[t_0, t_f]$ can be expressed by

$$\begin{aligned} E_{max}(\ell, \tau) &= \max_{t[k] \in [t_0, t_f]} E_k(\ell, \tau) = \\ &= \max_{0 \leq k \leq \lfloor (t_f - t_0)/\tau \rfloor} \|\mathfrak{q}^{\text{NS}}[k] - \mathfrak{q}^{\text{AS}}[k]\|. \end{aligned} \quad (65)$$

5.2 Analysis of Accuracy of EoEsqaQkdeLTI for LTI-QKDE

For the LTI-QKDE, we can obtain the AS to the equation (1) for constant $\boldsymbol{\omega}$. Since $\boldsymbol{\Omega}^2 = -\|\boldsymbol{\omega}\|^2 \mathbf{I}$ and $\hat{\boldsymbol{\Omega}} = \boldsymbol{\Omega} / \|\boldsymbol{\omega}\|$, Lemma 2 shows that

$$\begin{aligned} \mathfrak{q}(t[k+1]) &= \exp((t[k+1] - t[k])\boldsymbol{\Omega}/2) \mathfrak{q}(t[k]) \\ &= \left(\mathbf{I} \cos(\|\boldsymbol{\omega}\| \tau/2) + \hat{\boldsymbol{\Omega}} \sin(\|\boldsymbol{\omega}\| \tau/2) \right) \mathfrak{q}(t[k]). \end{aligned}$$

Therefore,

$$\mathfrak{q}[k+1] = \mathbf{G}_{\text{AS}}(k, \tau) \mathfrak{q}[k] \quad (66)$$

where

$$\begin{aligned} \mathbf{G}_{\text{AS}}(k, \tau) &= \mathbf{G}_k^{k+1}(\tau) = \mathbf{G}(\tau) = \exp(\tau \boldsymbol{\Omega}/2) \\ &= \mathbf{I} \cos(\|\boldsymbol{\omega}\| \tau/2) + \hat{\boldsymbol{\Omega}} \sin(\|\boldsymbol{\omega}\| \tau/2) \end{aligned} \quad (67)$$

is the AS to the transition matrix for any k . On the other hand,

$$\mathbf{G}_k^{k+1}(\ell, \tau) = \mathbf{G}(\ell, \tau) \quad (68)$$

for the LTI-QKDE. Consequently,

$$\begin{aligned} \mathbf{E}_{\mathcal{G}} &= \mathbf{G}(\tau) - \mathbf{G}(\ell, \tau) \\ &= \mathbf{I} \left[\cos \frac{\|\boldsymbol{\omega}\| \tau}{2} - \frac{1 - \alpha(\ell, c)}{1 + \alpha(\ell, c)} \right] \\ &\quad + \hat{\boldsymbol{\Omega}} \left[\sin \frac{\|\boldsymbol{\omega}\| \tau}{2} - \frac{\|\boldsymbol{\omega}\| \tau \beta(\ell, c)}{1 + \alpha(\ell, c)} \right] \end{aligned} \quad (69)$$

for any k . Let

$$x = \|\boldsymbol{\omega}\| \tau \quad (70)$$

then x must be a pure scalar parameter without any unit and we immediately have

$$\begin{cases} c = x^2/4, \\ \beta(\ell, c) = \beta(\ell, x^2/4), \\ \alpha(\ell, c) = c\beta(\ell, x)^2 = x^2[\beta(\ell, x^2/4)]^2/4. \end{cases} \quad (71)$$

Let

$$\begin{cases} f_1(\ell, x) = \cos \frac{x}{2} - \frac{1 - \frac{x^2}{4} [\beta(\ell, \frac{x^2}{4})]^2}{1 + \frac{x^2}{4} [\beta(\ell, \frac{x^2}{4})]^2}, \\ f_2(\ell, x) = \sin \frac{x}{2} - \frac{x\beta(\ell, \frac{x^2}{4})}{1 + \frac{x^2}{4} [\beta(\ell, \frac{x^2}{4})]^2}, \end{cases} \quad (72)$$

then

$$\mathbf{E}_{\mathcal{G}} = f_1(\ell, x) \mathbf{I} + f_2(\ell, x) \hat{\boldsymbol{\Omega}}. \quad (73)$$

Moreover,

$$\begin{aligned} \|\mathbf{E}_{\mathcal{G}}\| &= \left\| f_1(\ell, x) \mathbf{I} + f_2(\ell, x) \hat{\boldsymbol{\Omega}} \right\| \\ &\leq \|f_1(\ell, x) \mathbf{I}\| + \|f_2(\ell, x) \hat{\boldsymbol{\Omega}}\| \\ &= |f_1(\ell, x)| \|\mathbf{I}\| + |f_2(\ell, x)| \|\boldsymbol{\Omega}\| / \|\boldsymbol{\omega}\| \\ &= 2(|f_1(\ell, x)| + |f_2(\ell, x)|) \\ &= \mathcal{O}(x^{2\ell+1}) \\ &= \mathcal{O}(\tau^{2\ell+1}) \end{aligned} \quad (74)$$

for sufficiently small $x = \|\boldsymbol{\omega}\| \tau$ and any k . According to **Table 2** and (74), we can obtain **Table 4**. It is clear that the upper bound $2(|f_1(\ell, x)| + |f_2(\ell, x)|)$ for $\|\mathbf{E}_{\mathcal{G}}\|$ decreases rapidly when ℓ increases.

Furthermore, for the LTI-QKDE we have the single step computational error

$$\begin{aligned} \mathfrak{q}^{\text{AS}}[k+1] - \mathfrak{q}^{\text{NS}}[k+1] &= \mathbf{G}_{\text{AS}}(\tau) \mathfrak{q}^{\text{AS}}[k] - \mathbf{G}_{\text{NS}}(\tau) \mathfrak{q}^{\text{NS}}[k] \\ &= (\mathbf{G}_{\text{AS}}(\tau) - \mathbf{G}_{\text{NS}}(\tau)) \mathfrak{q}^{\text{AS}}[k] + \mathbf{G}_{\text{NS}}(\tau) (\mathfrak{q}^{\text{AS}}[k] - \mathfrak{q}^{\text{NS}}[k]) \end{aligned}$$

and its estimation

$$\begin{aligned} &\|\mathfrak{q}^{\text{AS}}[k+1] - \mathfrak{q}^{\text{NS}}[k+1]\| \\ &\leq \|(\mathbf{G}_{\text{AS}}(\tau) - \mathbf{G}_{\text{NS}}(\tau)) \mathfrak{q}^{\text{AS}}[k]\| + \|\mathbf{G}_{\text{NS}}(\tau) (\mathfrak{q}^{\text{AS}}[k] - \mathfrak{q}^{\text{NS}}[k])\| \\ &\leq \|\mathbf{G}_{\text{AS}}(\tau) - \mathbf{G}_{\text{NS}}(\tau)\| \|\mathfrak{q}^{\text{AS}}[k]\| + \|\mathbf{G}_{\text{NS}}(\tau)\| (\|\mathfrak{q}^{\text{AS}}[k] - \mathfrak{q}^{\text{NS}}[k]\|) \\ &= \|\mathbf{E}_{\mathcal{G}}\| + \|\mathfrak{q}^{\text{AS}}[k] - \mathfrak{q}^{\text{NS}}[k]\| \end{aligned}$$

since we have $\|\mathfrak{q}^{\text{AS}}[k]\| \equiv 1$ for any integer k and $\mathbf{G}_{\text{NS}}(\tau)$ is an orthogonal matrix. For $k=0$, we have

$$E_0(\ell, \tau) = \|\mathfrak{q}^{\text{AS}}[0] - \mathfrak{q}^{\text{NS}}[0]\| = 0$$

because of $\mathfrak{q}^{\text{AS}}[0] = \mathfrak{q}^{\text{NS}}[0] = \mathfrak{q}[0]$. In consequence,

$$\begin{aligned} E_k(\ell, \tau) &= \|\mathfrak{q}^{\text{AS}}[k] - \mathfrak{q}^{\text{NS}}[k]\| \\ &\leq \|\mathbf{E}_{\mathcal{G}}\| + E_{k-1}(\ell, \tau) \\ &\leq k \|\mathbf{E}_{\mathcal{G}}\| \end{aligned} \quad (75)$$

for any k by induction. Therefore,

$$\begin{aligned} E_{max}(\ell, \tau) &\leq 2k_{max} (|f_1(\ell, x)| + |f_2(\ell, x)|) \\ &= 2 \left\lfloor \frac{t_f - t_0}{\tau} \right\rfloor (|f_1(\ell, x)| + |f_2(\ell, x)|) \\ &= \mathcal{O}((t_f - t_0) \tau^{2\ell}). \end{aligned} \quad (76)$$

This implies that the maximum absolute error $E_{max}(\ell, \tau)$ has an upper bound with order $\mathcal{O}(\tau^{2\ell})$ for fixed value of $t_f - t_0$.

For the order parameter $\ell \in \{1, 2, \dots, 10\}$ and time step $\tau \in \{10^{-6}, 10^{-5}, 10^{-4}, 10^{-3}, 10^{-2}, 10^{-1}, 0.2, 0.4, 0.6, 0.8\}$ (seconds), **Figure 5** demonstrates the impacts of ℓ and τ on the maximum absolute error $E_{max}(\ell, \tau)$ for the LTI-QKDE.

Table 4: Accuracy of $\mathbf{G}(\ell, \tau)$ for LTI-QKDE: $\|\mathbf{E}_G\| \leq 2(|f_1(x)| + |f_2(x)|)$

ℓ	$f_1(\ell, x)$	$f_2(\ell, x)$	$2(f_1(x) + f_2(x)) = \mathcal{O}(x^{2\ell+1})$
1	$-\frac{x^4}{192} + \mathcal{O}(x^6)$	$\frac{x^3}{96} + \mathcal{O}(x^5)$	$\frac{x^3}{48} + \mathcal{O}(x^4) = \mathcal{O}(x^3)$
2	$-\frac{x^6}{46080} + \mathcal{O}(x^7)$	$\frac{x^5}{23040} + \mathcal{O}(x^7)$	$\frac{x^5}{11520} + \mathcal{O}(x^6) = \mathcal{O}(x^5)$
3	$-\frac{x^8}{25804800} + \mathcal{O}(x^{10})$	$\frac{x^7}{12902400} + \mathcal{O}(x^9)$	$\frac{x^7}{6451200} + \mathcal{O}(x^8) = \mathcal{O}(x^7)$
4	$-\frac{x^{10}}{26011238400} + \mathcal{O}(x^{12})$	$\frac{x^9}{13005619200} + \mathcal{O}(x^{11})$	$\frac{x^9}{6502809600} + \mathcal{O}(x^{10}) = \mathcal{O}(x^9)$
5	$-\frac{x^{12}}{41201801625600} + \mathcal{O}(x^{13})$	$\frac{x^{11}}{20600900812800} + \mathcal{O}(x^{12})$	$\frac{x^{11}}{10300450406400} + \mathcal{O}(x^{12}) = \mathcal{O}(x^{11})$

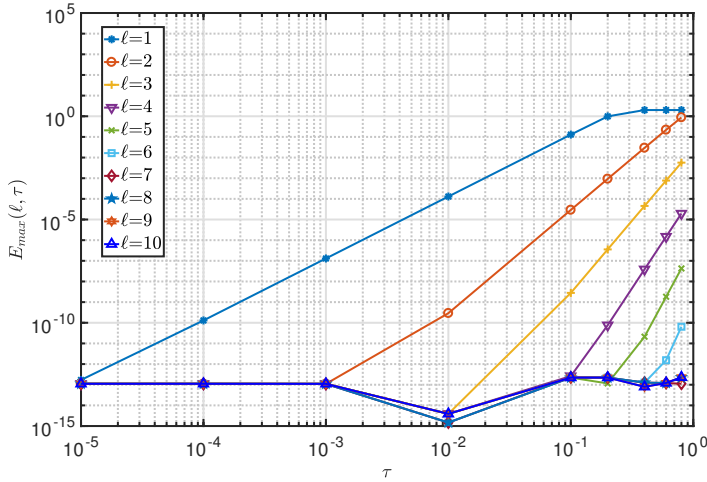
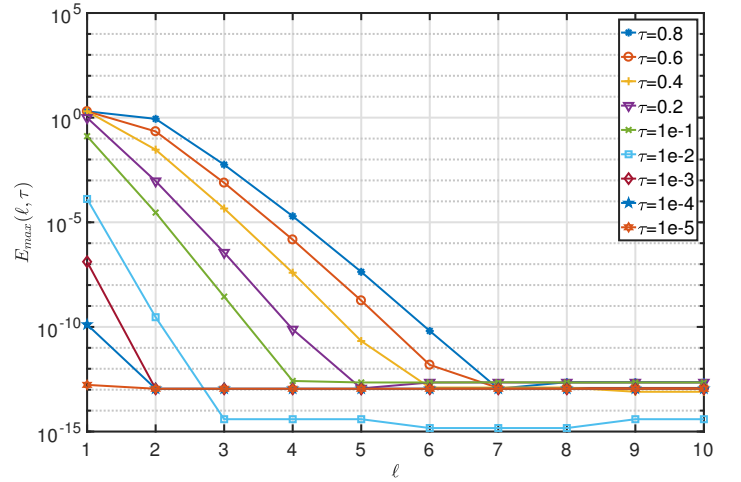

 (a) Effect of ℓ on $E_{max}(\ell, \tau)$ for fixed time step τ .

 (b) Effect of τ on $E_{max}(\ell, \tau)$ for fixed order parameter ℓ .

 Figure 5: $E_{max}(\ell, \tau)$ of LTI-QKDE for different order and time step with a long time span $[t_0, t_f] = [0, 2000]$, constant angular velocity $\boldsymbol{\omega} = \left[\pi \sin \frac{\pi}{8}, -\frac{\pi}{3} \cos \frac{\pi}{8}, -2 \sin \frac{\pi}{3} \right]^T$ and initial state $\mathbf{q}_0 = [1, 0, 0, 0]^T$.

Figure 5(a) shows that if $\tau \leq 10^{-3}$ second, we can set $\ell \geq 2$ since we have $E_{max}(\ell, \tau) \sim 10^{-13}$ for $\ell \geq 2$ instead of $E_{max}(\ell, \tau) \sim 10^{-7}$ for $\ell = 1$. If we set $E_{max}(\ell, \tau) \leq 10^{-5}$, we should set $\tau \leq 0.007$ second for $\ell = 1$ and $\tau \leq 0.11$ for $\ell \geq 2$. Moreover, for $\ell \geq 4$, $E_{max}(\ell, \tau)$ will be small enough which implies the time step can be set large enough ($0 < \tau < 1$) and the requirement for the performance of hardware will be easily satisfied.

about x -axis, θ is the pitch angle about y -axis, ϕ is the roll angle about z -axis. The Euler angles (ψ, θ, ϕ) can be converted to the quaternion $\mathbf{q} = [e_0, e_1, e_2, e_3]^T$ according to the following formula [10–12, 48]

5.3 Simulation of EoEsgaQkdeLTV for LTV-QKDE

5.3.1 Initial Value $\mathbf{q}[0]$ for the QKDE

The initial value $\mathbf{q}[0] = [e_0(t_0), e_1(t_0), e_2(t_0), e_3(t_0)]^T$ for the QKDE can be determined by the initial values of the Euler angles $\psi(t_0), \theta(t_0)$ and $\phi(t_0)$, where ψ is yaw angle

$$\begin{cases} e_0 = +\cos \frac{\psi}{2} \cos \frac{\theta}{2} \cos \frac{\phi}{2} + \sin \frac{\psi}{2} \sin \frac{\theta}{2} \sin \frac{\phi}{2}, \\ e_1 = +\cos \frac{\psi}{2} \cos \frac{\theta}{2} \sin \frac{\phi}{2} - \sin \frac{\psi}{2} \sin \frac{\theta}{2} \cos \frac{\phi}{2}, \\ e_2 = +\cos \frac{\psi}{2} \sin \frac{\theta}{2} \cos \frac{\phi}{2} + \sin \frac{\psi}{2} \cos \frac{\theta}{2} \sin \frac{\phi}{2}, \\ e_3 = -\cos \frac{\psi}{2} \sin \frac{\theta}{2} \sin \frac{\phi}{2} + \sin \frac{\psi}{2} \cos \frac{\theta}{2} \cos \frac{\phi}{2}. \end{cases} \quad (77)$$

Particularly, we have the two special configurations for the Euler angle and the quaternion, viz.

$$\begin{bmatrix} \psi \\ \theta \\ \phi \end{bmatrix} = \begin{bmatrix} 0 \\ \xi \\ 0 \end{bmatrix} \longleftrightarrow \mathbf{q}[0] = \begin{bmatrix} \cos \frac{\xi}{2} \\ 0 \\ \sin \frac{\xi}{2} \\ 0 \end{bmatrix} \quad (78)$$

and

$$\begin{bmatrix} \psi \\ \theta \\ \phi \end{bmatrix} = \begin{bmatrix} 0 \\ 0 \\ 0 \end{bmatrix} \longleftrightarrow \mathbf{q}[0] = \begin{bmatrix} 1 \\ 0 \\ 0 \\ 0 \end{bmatrix} \quad (79)$$

The equation (78) or (79) can be used to set the initial values $\mathbf{q}[0]$ for solving the attitudes.

5.3.2 A special LTV-QKDE with AS

For the constant parameters ω_0, ξ , initial state $\mathbf{q}[0]$ specified by (79) and the time-varying angular velocity

$$\boldsymbol{\omega}(t) = \begin{bmatrix} -\omega_0(1 - \cos \xi) \\ -\omega_0 \sin \xi \sin(\omega_0 t) \\ \omega_0 \sin \xi \cos(\omega_0 t) \end{bmatrix}, \quad (80)$$

it is easy to check that the corresponding AS to the LTV-QKDE is

$$\begin{aligned} \mathbf{q}^{\text{AS}}(t) &= [e_0(t), e_1(t), e_2(t), e_3(t)]^T \\ &= \left[\cos \frac{\xi}{2}, 0, \sin \frac{\xi}{2} \cos(\omega_0 t), \sin \frac{\xi}{2} \sin(\omega_0 t) \right]^T. \end{aligned}$$

For the discrete version, we have

$$\mathbf{q}^{\text{AS}}[k] = \mathbf{q}^{\text{AS}}(t_0 + k\tau) = \mathbf{G}_{k-1}^k(\tau) \mathbf{q}^{\text{AS}}[k-1].$$

On the other hand, the NS to the LTV-QKDE by the EOES-GAQKDELTV is

$$\begin{aligned} \mathbf{q}_{\ell, \tau}^{\text{NS}}[k] &= [e_0^{\text{NS}}[k], e_1^{\text{NS}}[k], e_2^{\text{NS}}[k], e_3^{\text{NS}}[k]]^T \\ &= \mathbf{G}_{k-1}^k(\ell, \tau) \mathbf{q}_{\ell, \tau}^{\text{NS}}[k-1]. \end{aligned} \quad (81)$$

Figure 6 demonstrates a numeric example of LTV-QKDE with AS. Here we set time span $t_f - t_0 = 2000$ seconds, $\omega_0 = 2\pi, \xi = \pi/80$, initial state $\mathbf{q}_0 = \mathbf{q}^{\text{AS}}(t_0)$ and $\boldsymbol{\omega}(t)$ according to (80). Obviously, larger order parameter ℓ implies smaller $E_{\max}(\ell, \tau)$ for fixed τ . If we set $\tau = 10^{-2}$ and need $E_{\max}(\ell, \tau) \sim 10^{-5}$, then any $\ell \geq 1$ is acceptable. However, if we set $\tau = 10^{-1}$ and $E_{\max}(\ell, \tau) \leq 10^{-5}$, then we should set $\ell \geq 2$. For $\ell \geq 4$ and $E_{\max}(\ell, \tau) \leq 10^{-4}$, a big step $\tau = 0.8$ is satisfactory. The figure shows that for fixed $E_{\max}(\ell, \tau)$, we can set large step for high order algorithms. In other words,

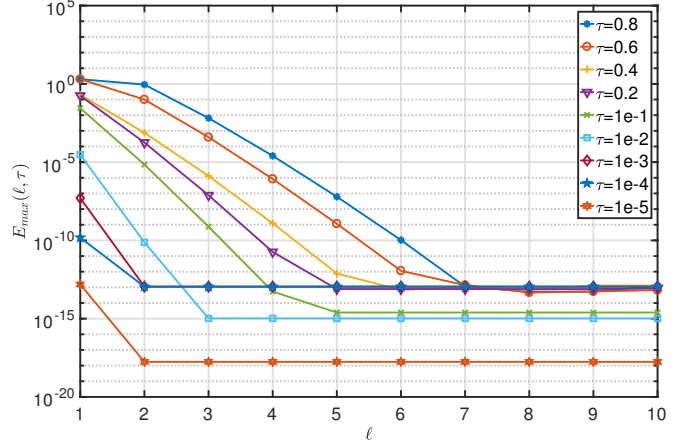


Figure 6: Effect of ℓ and τ on $E_{\max}(\ell, \tau)$ for LTV-QKDE

with configurable order parameter ℓ we can choose proper hardware for practical flight control systems by setting the step τ for sampling. Moreover, for fixed τ , a larger ℓ means better manoeuvrability in flight since it traces the variation of $\boldsymbol{\omega}(t)$ better. Obviously, this observation may be valuable for designing aircraft, spacecrafts, torpedoes and so on.

5.3.3 Simulation of LTV-QKDE with MATLAB Simulink

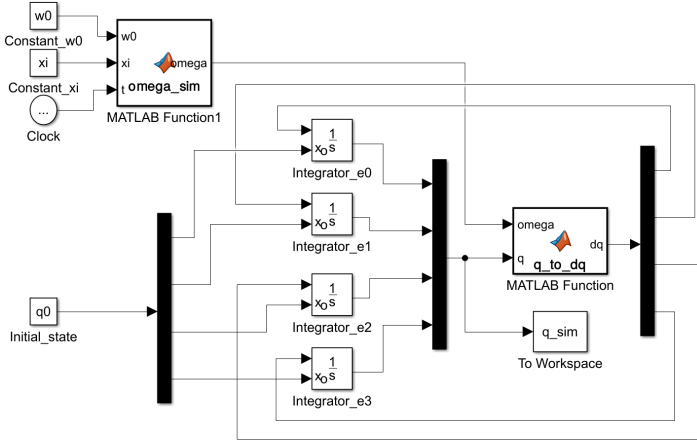
It is well known that there is no AS for a LTV system such as the LTV-QKDE. In addition to the NS, simulation is another method to explore the solution to LTV-QKDE.

Figure 7 illustrates the results of simulation for the LTV-QKDE. **Figure 7(a)** shows the diagram for simulating LTV-QKDE. **Figure 7(b)** demonstrates the error between the AS obtained by Simulink and the NS obtained by our SDS. Note that the error is represented by the $\|\mathbf{q}^{\text{sim}} - \mathbf{q}^{\text{NS}}\|$ for $\ell \in \{1, 2, 3, 4, 5\}$ with the time step $\tau = 10^{-5}$, the time span $[t_0, t_f] = [0, 100]$, the time-varying angular velocity $\boldsymbol{\omega}(t) = [-\omega_0 \cos(\xi t) \exp(-\omega_0 t), -\omega_0 \sin(\omega_0 t), \omega_0 \cos(\xi t) \cos(\omega_0 t)]^T$, and the initial state \mathbf{q}_0 determined by (79) such that $\omega_0 = 2\pi$ and $\xi = \pi/80$.

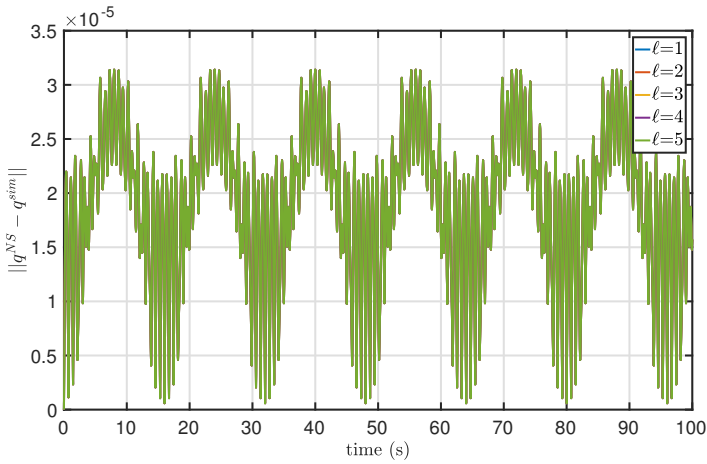
5.4 Discussion

For the purpose of verification and validation, our emphasis is put on numerical simulation and system simulation since strict mathematical proofs and analysis are provided in this paper. For the readers who cares about real-world or benchmark problems, please see [11], [12] and so on. This work is a big extension of [35], thus the comparison of SDS and traditional difference scheme is omitted. We remark that the adaptive step size method [49] is not considered since it increases the complexity when implementing the SDS with hardware due to the fixed sampling frequency of IMU and it is not symplectic.

Our work is based on the single step numerical method driven by the real-time computation and hardware imple-



(a) MATLAB Simulink diagram.



(b) Error between Pseudo AS to LTV-QKDE and NS with MATLAB Simulink

Figure 7: Simulation with MATLAB Simulink

mentation. The multiple steps method is not considered in this paper. The typical multiple steps method is the *triple-jump composition* method popularized by Creutz [50], Yosida [51] and Suzuki [52]. Furthermore, Yosida’s symplectic method is based on the separability of the Hamiltonian which is not satisfied for the QKDE, neither Suzuki’s method nor Creutz’s method is symplectic.

We also remark that the computational costs of division operation and multiplication are not the same in general. However, the analysis of computational cost with the time complexity vector of computation $\mathbf{u} = [u_+, u_*, u_\div] = [u_1, u_2, u_3]$ instead of $\mathbf{u} = [u_+, u_*] = [u_1, u_2]$ will lead to the same computational complexity. In consequence, it is enough to consider the addition and multiplication for the operations of float numbers. The essence lies in whether there are nested loops or not in the algorithms instead of the difference of division and multiplication.

6 Conclusions

The essential observations for solving the QKDE with high order ESGA include four aspects:

- the general LTV-QKDE can be modeled by the linear Hamiltonian system with infinitesimal symplectic structure;
- the symplectic Padé approximation can be used to construct the SDS for QKDE with 2ℓ -th order accuracy;
- the symplectic transform (single-step transition operator) can be simplified by the Padé-Cayley lemma;
- the parameters for the SDS can be obtained with parallel and alternative iterative methods;

The performance of algorithms — EoESGAQKDELTV and EoESGAQKDELTI — are attractive due to the following reasons:

- there are no accumulative computational errors in the sense of long term time since they are symplectic;
- the order parameter ℓ is configurable, which benefits the designer of practical engineering systems such as aircraft, spacecrafts and so on according to the acceptable angular velocity;
- the time complexity of computation for the algorithms proposed is linear while the space complexity of computation is constant, thus our algorithms are appropriate for real-time applications;
- the maximum absolute error when solving the LTI-QKDE is controlled by the time span $t_f - t_0$, time step τ and the order parameter ℓ through the relation $E_{max}(\ell, \tau) = \mathcal{O}((t_f - t_0)\tau^{2\ell})$, and the simulation result shows that this relation also holds for some LTV-QKDE.

Since the LTI-QKDE is a special case of LTV-QKDE and the EoESGAQKDELTV surpasses the algorithms ESGA-I and ESGA-II proposed in [35], it is enough for us to use the EoESGAQKDELTV algorithm for solving QKDE. Generally, $\ell = 2$ is enough (which means fourth order precision) for the applications with low speed and $\ell = 5$ is enough (which means tenth order precision) for the applications with high speed.

Acknowledgement

Our thanks go for Dr. Zi-Hao Wang for his help in simulation of LTV-QKDE with MATLAB Simulink demonstrated in **Figure 7**.

Code Availability Statement

The code for the algorithms appeared in this paper have been released on the following GitHub site:

<https://github.com/GrAbsRD/EoESGA>

A Hamiltonian System

W. R. Hamilton introduced the canonical differential equations [53, 54]

$$\frac{d p_i}{d t} = -\frac{\partial H}{\partial q_i}, \quad \frac{d q_i}{d t} = \frac{\partial H}{\partial p_i}, \quad i = 1, 2, \dots, N$$

for problems of geometrical optics, where p_i are the generalized momentum, q_i are the generalized displacements and $H = H(p_1, \dots, p_N, q_1, \dots, q_N)$ is the Hamiltonian, viz., the total energy of the system. Let $\mathbf{p} = [p_1, \dots, p_N]^\top \in \mathbb{R}^{N \times 1}$, $\mathbf{q} = [q_1, \dots, q_N]^\top \in \mathbb{R}^{N \times 1}$, and $\mathbf{z} = [p_1, \dots, p_N, q_1, \dots, q_N]^\top = [\mathbf{p}^\top, \mathbf{q}^\top]^\top \in \mathbb{R}^{2N \times 1}$, then $H = H(\mathbf{p}, \mathbf{q}) = H(\mathbf{z})$ can be specified by \mathbf{z} in the $2N$ -dimensional phase space. Since the gradient of H is

$$H_{\mathbf{z}} = \left[\frac{\partial H}{\partial p_1}, \dots, \frac{\partial H}{\partial p_N}, \frac{\partial H}{\partial q_1}, \dots, \frac{\partial H}{\partial q_N} \right]^\top \in \mathbb{R}^{2N \times 1}.$$

Then the canonical equation is equivalent to

$$\frac{d \mathbf{z}}{d t} = \mathbf{J}_{2N}^{-1} \cdot H_{\mathbf{z}}(\mathbf{z}), \quad \mathbf{J}_{2N} = \begin{bmatrix} \mathbf{O}_N & \mathbf{I}_N \\ -\mathbf{I}_N & \mathbf{O}_N \end{bmatrix} \quad (82)$$

where \mathbf{I}_N is the N -by- N identical matrix, \mathbf{O}_N is the N -by- N zero matrix and \mathbf{J}_{2N} is the $2N$ -th order standard symplectic matrix [44, 55]. For simplicity, the subscripts in \mathbf{I}_N , \mathbf{I}_{2N} and \mathbf{J}_{2N} may be omitted. Any system which can be described by (82) is called an *Hamiltonian system*. There are some fundamental properties for the canonical equation of Hamiltonian system [53, 56–58]:

- (i) it is invariant under the symplectic transform (phase flow);
- (ii) the evolution of the system is the evolution of symplectic transform;
- (iii) the symplectic symmetry and the total energy of the system can be preserved simultaneously and automatically.

B Cayley Transform and Its Mirror

The Cayley transform is defined by [59]

$$\varphi(z) = \frac{1-z}{1+z}, \quad z \in \mathbb{C} \quad (83)$$

which is introduced by Cayley original and developed by Weyl [60] in 1940s as well as by Wu [61] in 2009. The complex variable $z \in \mathbb{C} \setminus \{-1\}$ in (83) can be generalized to the matrix form, viz. [60]

$$\varphi(\mathbf{A}) = \frac{\mathbf{I} - \mathbf{A}}{\mathbf{I} + \mathbf{A}}, \quad \mathbf{A} \in \mathbb{R}^{n \times n} \quad (84)$$

such that $\mathbf{I} + \mathbf{A} \in \text{GL}(n, \mathbb{R}) = \{\mathbf{B} \in \mathbb{R}^{n \times n} : \det(\mathbf{B}) \neq 0\}$ where $\frac{\mathbf{I} - \mathbf{A}}{\mathbf{I} + \mathbf{A}}$ denotes the multiplication $(\mathbf{I} - \mathbf{A})(\mathbf{I} + \mathbf{A})^{-1} = (\mathbf{I} + \mathbf{A})^{-1}(\mathbf{I} - \mathbf{A})$. Although there are various properties of Cayley transform [60, 61], we just list the following theorem according to our purpose in this paper :

Theorem 9. *For the non-exceptional matrix $\mathbf{A} \in \mathbb{R}^{n \times n}$, i.e. $\mathbf{I} + \mathbf{A} \in \text{GL}(n, \mathbb{R})$, the following statements hold:*

- i) if λ is the eigenvalue of \mathbf{A} such that $\mathbf{A}\mathbf{p} = \lambda\mathbf{p}$, then $\varphi(\lambda)$ is the eigenvalue of $\varphi(\mathbf{A})$, viz. $\varphi(\mathbf{A})\mathbf{p} = \varphi(\lambda)\mathbf{p}$;
- ii) if $\forall n \in \mathbb{N}$, then $\varphi^{2n}(\mathbf{A}) = \mathbf{A}$, $\varphi^{2n-1}(\mathbf{A}) = \varphi(\mathbf{A})$;
- iii) if $\mathbf{A} \in \text{GL}(n, \mathbb{R})$, then $\varphi(\mathbf{A}^{-1}) = -\varphi(\mathbf{A})$;
- iv) if $\varphi(\mathbf{A}) \in \text{GL}(n, \mathbb{R})$, then $\varphi(\mathbf{A})^{-1} = \varphi(-\mathbf{A})$;
- v) $\varphi(\mathbf{A}) = 2(\mathbf{I} + \mathbf{A})^{-1} - \mathbf{I} = -2\mathbf{A}(\mathbf{I} + \mathbf{A})^{-1} + \mathbf{I}$;

The matrix transform

$$\varphi_{\text{mct}}(\mathbf{A}) = \varphi(-\mathbf{A}), \quad (85)$$

it is called the *mirrored Cayley transform* of \mathbf{A} . Obviously, for the non-exceptional matrix $\mathbf{A} \in \mathbb{R}^{n \times n}$ such that $\mathbf{I} \pm \mathbf{A} \in \text{GL}(n, \mathbb{R})$ are invertible, we have

$$\begin{aligned} \varphi_{\text{mct}}(\mathbf{A}) &= \frac{\mathbf{I} + \mathbf{A}}{\mathbf{I} - \mathbf{A}} \\ &= (\mathbf{I} + \mathbf{A})(\mathbf{I} - \mathbf{A})^{-1} \\ &= (\mathbf{I} - \mathbf{A})^{-1}(\mathbf{I} + \mathbf{A}) \end{aligned} \quad (86)$$

C Horner's Rule for Computing Polynomials

For the polynomial $p_s(x) = \sum_{i=0}^s c_i x^i = c_0 + c_1 x + \dots + c_s x^s$ we have the **Algorithm 7** based on Horner's rule for computing this polynomial with computational complexity $\mathcal{O}(s)$.

Algorithm 7 Computing Polynomials by Horner's Rule

Input: The degree s , coefficients c_0, c_1, \dots, c_s and variable x of the polynomial to be calculated.

Output: $p_s(x) = \sum_{i=0}^s c_i x^i$

- 1: **function** POLYNOMIAL(c_0, \dots, c_s, x)
- 2: $T \leftarrow c_s$;
- 3: **for** $i \in \langle 1, 2, \dots, s \rangle$ **do**

```

4:      $T \leftarrow T \cdot x + c_{s-i}$ ;
5:   end for
6:   return  $T$ ;
7: end function

```

References

- [1] Bong Wie and Peter M Barba. Quaternion feedback for spacecraft large angle maneuvers. *Journal of Guidance, Control, and Dynamics*, 8(3):360–365, May 1985.
- [2] Bong Wie, H Weiss, and A Arapostathis. Quaternion feedback regulator for spacecraft eigenaxis rotations. *Journal of Guidance, Control, and Dynamics*, 12(3):375–380, May 1989.
- [3] Bong Wie and Jianbo Lu. Feedback control logic for spacecraft eigenaxis rotations under slew rate and control constraints. *Journal of Guidance, Control, and Dynamics*, 18(6):1372–1379, Nov. 1995.
- [4] Bong Wie, David Bailey, and Christopher Heiberg. Rapid multitarget acquisition and pointing control of agile spacecraft. *Journal of Guidance, Control, and Dynamics*, 25(1):96–104, Jan. 2002.
- [5] J Kuipers. *Quaternions and Rotation Sequences: A Primer with Applications to Orbits, Aerospace and Virtual Reality*. Princeton University Press, 2002.
- [6] Bernard Friedland. Analysis strapdown navigation using quaternions. *IEEE Transactions on Aerospace and Electronic Systems*, AES-14(5):764–768, Sept. 1978.
- [7] Anthony Kim and MF Golnaraghi. A quaternion-based orientation estimation algorithm using an inertial measurement unit. In *Position Location and Navigation Symposium, 2004. PLANS 2004*, pages 268–272. IEEE, Apr. 2004.
- [8] R.M. Rogers. *Applied Mathematics in Integrated Navigation Systems*. AIAA, Reston, 2007.
- [9] Yong Min Zhong, She Sheng Gao, and Wei Li. A quaternion-based method for SINS/SAR integrated navigation system. *IEEE Transactions on Aerospace and Electronic Systems*, 48(1):514–524, Jan. 2012.
- [10] Joseph M Cooke, Michael J Zyda, David R Pratt, and Robert B McGhee. NPSNET: Flight simulation dynamic modeling using quaternions. *Presence: Teleoperators & Virtual Environments*, 1(4):404–420, 1992.
- [11] David Allerton. *Principles of flight simulation*. John Wiley & Sons, 2009.
- [12] Dominic J Diston. *Computational Modelling and Simulation of Aircraft and the Environment, Volume 1: Platform Kinematics and Synthetic Environment*. John Wiley & Sons, 2009.
- [13] Jon S. Berndt, Tony Peden, and David Megginson. JSBSim, open source flight dynamics software library. <http://jsbsim.sourceforge.net/>, access date: July 1, 2024.
- [14] J. S. Yuan. Closed-loop manipulator control using quaternion feedback. *IEEE Journal on Robotics and Automation*, 4(4):434–440, Aug. 1988.
- [15] Janez Funda, Russell H Taylor, and Richard P Paul. On homogeneous transforms, quaternions, and computational efficiency. *IEEE Transactions on Robotics and Automation*, 6(3):382–388, Jun. 1990.
- [16] Jack CK Chou. Quaternion kinematic and dynamic differential equations. *IEEE Transactions on Robotics and Automation*, 8(1):53–64, Feb. 1992.
- [17] O-E Fjellstad and Thor I Fossen. Position and attitude tracking of AUV’s: A quaternion feedback approach. *IEEE Journal of Oceanic Engineering*, 19(4):512–518, Oct. 1994.
- [18] Mohammad Zamani, Jochen Trumppf, and Robert Mahony. Minimum-energy filtering for attitude estimation. *IEEE Transactions on Automatic Control*, 58(11):2917–2921, Nov. 2013.
- [19] Raul Murartal, J. M. M. Montiel, and Juan D. Tardos. ORB-SLAM: A Versatile and Accurate Monocular SLAM System. *IEEE Transactions on Robotics*, 31(5):1147–1163, 2015. arXiv:1502.00956v2 [cs.RO].
- [20] CH Robotics content library: Understanding quaternions. Online. <http://www.chrobotics.com/library/understanding-quaternions>, access date: Aug. 1, 2021.
- [21] Richard Szeliski. *Computer Vision: Algorithms and Applications*. Texts in Computer Science. Springer, London, 2010. Available on line: <http://szeliski.org/Book/>.
- [22] John Vince. *Quaternions for Computer Graphics*. Springer, London, 2011.
- [23] Kit Ian Kou and Yong-Hui Xia. Linear quaternion differential equations: Basic theory and fundamental results. *Studies in Applied Mathematics*, 141(1):3–45, 2018. arXiv:1510.02224v5 [math.CA]. available at: <https://arxiv.org/abs/1510.02224>.
- [24] Alit Kartiwa, Asep K. Supriatna, Endang Rusyaman, and Jumat Sulaiman. Review of quaternion differential equations: Historical development, applications, and future direction. *Axioms*, 12(5):article–number 483, 2023.
- [25] Alfred C Robinson. On the use of quaternions in simulation of rigid-body motion. Technical Report AD-0234422, Wright Air Development Center, Chicago, Dec. 1958.

- [26] John Hrastar. Attitude control of a spacecraft with a strapdown inertial reference system and onboard computer. Technical Report NASA-TN-D-5959, NASA, Sept. 1970.
- [27] David C Cunningham, Thomas P Gismondi, and George W Wilson. Control system design of the annular suspension and pointing system. *Journal of Guidance Control Dynamics*, 3:11–21, May. 1980.
- [28] Julyan H. E. Cartwright and Oreste Piro. The dynamics of Runge–Kutta methods. *International Journal of Bifurcation and Chaos*, 2:427–449, 1992. Available online. <http://het.physics.ntua.gr/~konstant/ph36/doc/CartwrightAndPiroRKpaper.pdf>.
- [29] Wolfram Mathworld. Runge-Kutta method. Online, May 11, 2024. <https://mathworld.wolfram.com/Runge-KuttaMethod.html>.
- [30] W. H. Press, B. P. Flannery, S. A. Teukolsky, and W. T. Vetterling. *Numerical Recipes in FORTRAN: The Art of Scientific Computing*, chapter 16, pages 704–716. Cambridge University Press, Cambridge, England, 2nd edition, 1992. Please see §16.1 "Runge-Kutta Method" and §16.2 "Adaptive Step Size Control for Runge-Kutta."
- [31] ShunJin Wang and Hua Zhang. Algebraic dynamics algorithm: Numerical comparison with Runge-Kutta algorithm and symplectic geometric algorithm. *Science in China Series G: Physics Mechanics and Astronomy*, 50(1):53–69, Feb. 2007.
- [32] John C Butcher. Implicit Runge-Kutta processes. *Mathematics of Computation*, 18(85):50–64, Jan, 1964.
- [33] Arieh Iserles. *A First Course in the Numerical Analysis of Differential Equations*. Cambridge University Press, 1996.
- [34] James M Varah. On the efficient implementation of implicit Runge-Kutta methods. *Mathematics of Computation*, 33(146):557–561, 1979.
- [35] Hong-Yan Zhang, Zi-Hao Wang, Lu-Sha Zhou, Qian-Nan Xue, Long Ma, and Yi-Fan Niu. Explicit symplectic geometric algorithm for quaternion kinematical differential equation. *IEEE/CAA Journal of Automatica Sinica*, 5(2):479–488, Mar. 2018.
- [36] Pieter Simke de Vries, Jim Rojer, and Floris E. Kalf. Quantum-based relative inertial navigation with velocity-aided alignment and initialization. *Engineering Proceedings*, 54(1):39(1–10), 2023. <https://www.mdpi.com/2673-4591/54/1/39>.
- [37] Hayley Dunning and Thomas Angus. Quantum sensor for a future navigation system tested aboard royal navy ship, 2023. Available online. <https://www.imperial.ac.uk/news/245114/quantum-sensor-future-navigation-system-tested/>.
- [38] Advanced Navigation. The future of inertial navigation is classical-quantum sensor fusion, 2024. Available online. <https://www.advancednavigation.com/tech-articles/the-future-of-inertial-navigation-is-classical-quantum>.
- [39] Zhen Feng Cai and Kit Ian Kou. Solving quaternion ordinary differential equations with two-sided coefficients. *Qualitative Theory of Dynamical Systems*, 17:441–462, 2018.
- [40] A. Kameli Donachali and H. Jafari. Decomposition method for solving quaternion differential equations. *International Journal of Applied and Computational Mathematics*, 6(4):e107, 2020.
- [41] Jie Liu, Siyu Sun, and Zhibo Cheng. Boundary value problems of quaternion-valued differential equations: solvability and green’s function. *Boundary Value Problems*, pages article–number 113(2023), 2023.
- [42] George A. Baker. *Padé Approximants*. Cambridge University Press, London, 2nd edition, 1996.
- [43] Annie Cuyt. *Padé Approximants for Operators: Theory and Applications*. Springer Berlin, Heidelberg, 1984.
- [44] Kang Feng and Mengzhao Qin. *Symplectic Geometric Algorithms for Hamiltonian systems*. Springer, 2010.
- [45] Jiu-Shao Qin. Introduction to jiu-shao qin. Available from https://mathshistory.st-andrews.ac.uk/Biographies/Qin_Jiushao/.
- [46] Allan Borodin. *Horner’s Rule is Uniquely Optimal*, pages 45–58. Academic Press, 12 1971. In book: Theory of Machines and Computations.
- [47] Donald E. Knuth. *The Art of Computer Programming: Seminumerical Algorithms*, pp. 467–469, 1998., volume 2. Addison-Wesley, 3rd edition, 1998.
- [48] Soohwan Kim and Minkyung Kim. Rotation representations and their conversions. *IEEE Access*, 11(1):6682–6699, 2023.
- [49] L. M. Skvortsov. Explicit adaptive Runge-Kutta methods. *Mathematical Models and Computer Simulations*, 4(1):82–91, 2012.
- [50] Michael Creutz and Andreas Gocksch. Higher-order hybrid Monte Carlo algorithms. *Physics Review Letter*, 63:9–12, Jul 1989.
- [51] Haruo Yoshida. Construction of higher order symplectic integrators. *Physics Letters A*, 150(5):262–268, 1990.
- [52] Masuo Suzuki. Fractal decomposition of exponential operators with applications to many-body theories and Monte Carlo simulations. *Physics Letters A*, 146:319–323, 1990.

- [53] Vladimir I Arnold. *Mathematical Methods of Classical Mechanics*, volume 60 of *Graduate Texts in Mathematics*. Springer, Apr. 1989.
- [54] Vladimir I Arnold, Valery V Kozlov, and Anatoly I Neishtadt. *Mathematical Aspects of Classical and Celestial Mechanics*, volume 3. Springer, 2007.
- [55] Kang Feng. On difference schemes and symplectic geometry. In *Proceeding of the 1984 Beijing Symposium on differential geometry and differential equations.*, pages 42–58. Science Press, 1984.
- [56] Ling Hua Kong, Jia Lin Hong, Lan Wang, and Fang Fang Fu. Symplectic integrator for nonlinear high order Schrödinger equation with a trapped term. *Journal of computational and applied mathematics*, 231(2):664–679, Sept. 2009.
- [57] JM Franco and I Gómez. Construction of explicit symmetric and symplectic methods of Runge–Kutta–Nyström type for solving perturbed oscillators. *Applied Mathematics and Computation*, 219(9):4637–4649, Jan. 2013.
- [58] David M Hernandez. Fast and reliable symplectic integration for planetary system N-body problems. *Monthly Notices of the Royal Astronomical Society*, 458(4):4285–4296, Jun. 2016.
- [59] Walter Rudin. *Real Analysis and Complex Analysis*. McGraw-Hill, 3rd edition, 1987.
- [60] H. Weyl. *The Classic Groups: their invariants and representations*. Princeton University Press, New Jersey, 1946.
- [61] F.-C. Wu, Z.-H. Wang, and Z.-Y.Hu. Cayley transformation and numerical stability of calibration equation. *International Journal of Computer Vision*, 82(2):156–184, 2009.